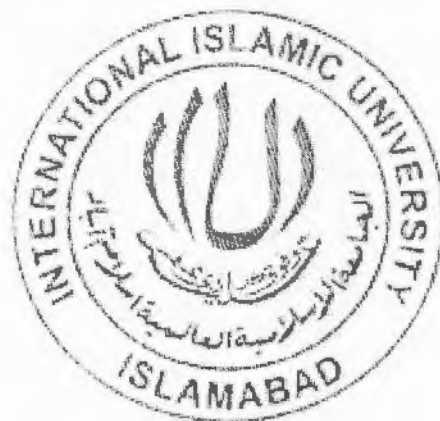


**Temperature dependent magnetic properties of
uncoated and SiO₂ coated CoCr₂O₄ nanoparticles**



by:

Ghazanfar Mehboob
(340-FBAS/MSPHY/F15)

Supervisor:

Dr. Kashif Nadeem

Assistant Professor

Department of Physics, FBAS,

IIUI, Islamabad

Department of Physics

Faculty of Basic and Applied Sciences

International Islamic University, Islamabad

(2017)



Accession No TH:18367 *Wm*

*MIS
620.5
GHT*

*Nanotechnology
Nanoparticles
X-Ray Diffraction*

**Temperature dependent magnetic properties of
uncoated and SiO₂ coated CoCr₂O₄ nanoparticles**

by:

Ghazanfar Mehboob

(340-FBAS/MSPHY/F15)

This Thesis submitted to Department of Physics International Islamic
University Islamabad, for the award of degree of
MS Physics.



CHAIRMAN
DEPT. OF PHYSICS
International Islamic University
Islamabad

**Chairman, Department of Physics
International Islamic University, Islamabad**



**Dean Faculty of Basic and Applied Science
International Islamic University, Islamabad**

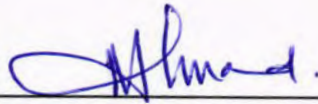
**Department of Physics
Faculty of Basic and Applied Sciences
International Islamic University, Islamabad**

Final Approval

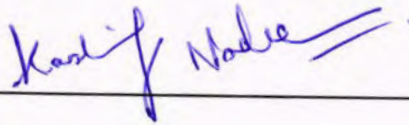
It is certified that the work printed in this thesis entitled "Temperature Dependent Magnetic Properties of Uncoated and SiO_2 Coated CoCr_2O_4 Nanoparticles" by Ghazanfar Mehboob, registration No.340-FBAS/ MSPHY/ F15 is of sufficient standard in scope and quality for award of degree of MS Physics from Department of Physics, International Islamic University, Islamabad, Pakistan.

Viva Voce Committee

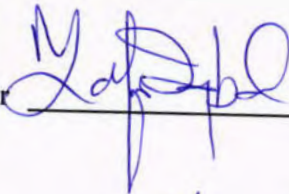
Chairman (Physics)



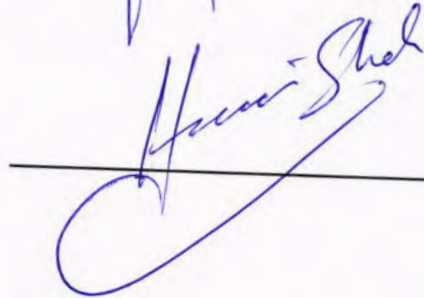
Supervisor



External Examiner



Internal Examine

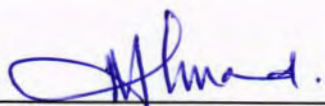


Final Approval

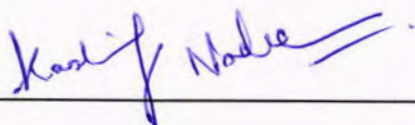
It is certified that the work printed in this thesis entitled "Temperature Dependent Magnetic Properties of Uncoated and SiO₂ Coated CoCr₂O₄ Nanoparticles" by Ghazanfar Mehboob, registration No.340-FBAS/ MSPHY/ F15 is of sufficient standard in scope and quality for award of degree of MS Physics from Department of Physics, International Islamic University, Islamabad, Pakistan.

Viva Voce Committee

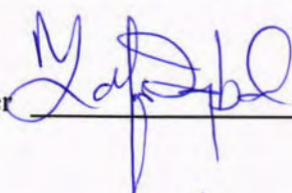
Chairman (Physics)



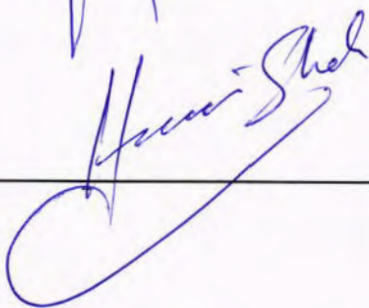
Supervisor



External Examiner



Internal Examine





DEDICATED

to

My beloved

Mother

Father

and

My

Respected teachers

Declaration

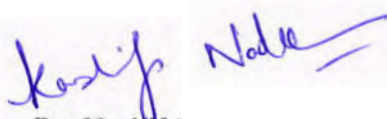
I **Ghazanfar Mehboob** (Registration # 340-FBAS/MSPHY/F15) student of MS in Physics (session 2015-2017), here declare that the matter printed in the thesis titled “**Temperature dependent magnetic properties of uncoated and SiO₂ coated CoCr₂O₄ nanoparticles**” is my own work and has not been published or submitted as research work or thesis in any form in any other university or institute in Pakistan or abroad.

Ghazanfar Mehboob
(340-FBAS/MSPHY/F15)

Dated: _____

Forwarding Sheet by Research Supervisor

The thesis entitled “Temperature dependent magnetic properties of uncoated and SiO₂ coated CoCr₂O₄ nanoparticles” submitted by Ghazanfar Mehboob (Registration No. 340-FBAS/MSPHY/F15) in partial fulfillment of M.S. degree in Physics has been completed under my guidance and supervision. I am satisfied with the quality of student’s research work and allow him to submit this thesis for further process to graduate with Master of Science degree from Department of Physics, as per IIU rules and regulations.



Dr. Kashif Nadeem

Assistant Professor

Department of Physics,
International Islamic University,
Islamabad.

Dated: _____

Acknowledgment

First, I owe my deepest gratitude to **Allah** Almighty for all of his countless blessings. I offer my humblest words of thanks to HIS most noble messenger **Hazrat Muhammad (P.B.U.H)**, who is forever, a torch of guidance and knowledge for all humanity. By virtue of his blessings today I am able to carry out our research work and present it.

I would like to acknowledge the worth mentioning supervision of **Dr. Kashif Nadeem** who guided me and supported me during my whole research work. Without his guidance it was not possible for me to complete my **MS**. Almighty **Allah** blessed them in every part of life.

I especially want to acknowledge my brothers **Qaisir Mehboob, Mudassar Mehboob, Gohar Mehboob** and my friend **Shahnawaz Sikandar** for their encouragement, support and confidence on me. During my education career their personality will remain the role model for me. Finally I am thankful to my **parents** and **sisters** for their love, care and support in my life, which has been directly encouraging me for my study. My parents' prayers have always been a big support in solving my problems. Allah may bless my parents and family with long life, health and happiness. I also pay special thanks to **Muhammad Kamran, Faisal Zeb, Aqib Javed, Syed Zaeem ul Hassan, Irfan Ahmed, Ziafat Ali Shah, Waheed Riaz, Waqas Shoukat** and special thanks to **Mr. Noman Saeed**. Who supported me during my research work. It was impossible to complete this work without their efforts.

Ghazanfar Mehboob
(340-FBAS/MSPHY/F15)

Contents

CHAPTER 1	1
INTRODUCTION.....	1
1.1 Nanoscience.....	1
1.1.1 Nanotechnology.....	1
1.1.2 Nano-meter Scale.....	1
1.1.3 Unique Properties of Nanomaterials.....	3
1.1.4 Nanomaterials and their Classification.....	4
1.1.5 Zero-Dimensional Nanomaterials.....	5
1.1.6 One- Dimensional Nanomaterials.....	5
1.1.7 Two-Dimensional Nanomaterials.....	5
1.1.8 Applications of Nanomaterials.....	6
1.2 Magnetism.....	7
1.2.1 Origin of Magnetism.....	9
1.2.2 Magnetism by Nucleus.....	9
1.3 Classification of magnetic material.....	9
1.3.1 Diamagnetism.....	10
1.3.2 Paramagnetism.....	12
1.3.3 Ferromagnetism.....	13
1.3.4 Anti-ferromagnetism.....	14
1.3.5 Ferrimagnetism.....	15
1.4 Superparamagnetism.....	16
1.4.1 Blocking Temperature.....	16
1.4.2 Neel Theory.....	17
1.4.3 Curie Temperature.....	17
1.5 Hysteresis.....	18
1.5.1 Saturation Magnetization.....	19
1.5.2 Remanent Magnetization.....	20
1.5.3 Coercivity.....	20
1.6 Chromites.....	20
1.6.1 Structure of Chromites.....	21
1.6.2 Cobalt Chromite (CoCr_2O_4).....	21

1.6.3	Effect of SiO ₂ surface coating.....	22
CHAPTER 2		23
LITERATURE REVIEW.....		23
2.1	Literature Review.....	23
CHAPTER 3		27
SYNTHESIS AND CHARACTERIZATION TECHNIQUES.....		27
3.1	Fabrication Techniques of Nanomaterial.....	27
3.1.1	Top Down Approach	27
3.1.2	Bottom Up Approach	27
3.2	Synthesis of CoCr ₂ O ₄ /SiO ₂ Nanoparticles.....	28
3.3	Characterization Techniques.....	30
3.4	Transmission Electron Microscopy	31
3.4.1	Working Principle of TEM	31
3.5	X-Ray Diffraction (XRD)	32
3.5.1	Basic Principle of XRD.....	33
3.5.2	Bragg's Law	34
3.5.3	Applications of X-rays.....	35
3.6	Superconducting Quantum Interference Device (SQUID) Magnetometer	36
CHAPTER 4		39
RESULTS AND DISCUSSION		39
4.1	X-Ray Diffraction	39
4.2	Transmission Electron Microscope	41
4.3	Zero Field Cooled-Field Cooled Magnetization.....	41
4.4	T-dependent M-H Loops of Uncoated Nanoparticles.....	44
4.4.1	T-dependent M-H Loops of SiO ₂ Coated Nanoparticles.....	47
4.4.2	H _c and M _s for Uncoated and Silica Coated Nanoparticles.....	49
4.5	Kneller's Law fitting.....	51
Conclusions		53
References		54

List of Figures

Fig. 1.1: Size of different objects at nanometre range.	2
Fig. 1.2: Gold and silver particles in glass.....	2
Fig. 1.3: Ratio of surface area-to-volume of structure and quantum mechanical effects.....	4
Fig. 1.4: 0- dimensional, 1-Dimensional, 2-Dimensional and 3-Dimensional nanomaterial.....	6
Fig. 1.5: Practical applications of nanotechnology.	7
Fig. 1.6: Spin and orbital motion in an atom.	9
Fig. 1.7: Magnetic behaviour of material.....	10
Fig. 1.8: Diamagnetic material in presence of field and zero field.....	11
Fig. 1.9: Diamagnetic material behaviour with temperature and magnetic field.....	12
Fig. 1.10: Behaviour of paramagnetic material with and without applied magnetic field.....	13
Fig. 1.11: Paramagnetic material behaviour with temperature and magnetic field.....	13
Fig. 1.12: Ferromagnetism Behaviour (a) In The Absence Of Magnetic Field (b) When Magnetic Field Is Applied.	14
Fig. 1.13: order of magnetic moments in anti-ferromagnetic materials.....	15
Fig. 1.14: Anti-parallel alignment of ferrimagnetism.	16
Fig. 1.15: Temperature effect on magnetic material.....	18
Fig. 1.16: Flow of current through coil.....	19
Fig. 1.17: Hysteresis loop of ferromagnetic material.....	20
Fig. 1.18: Crystal Structure of Spinel Chromite.	21
Fig. 3.1: Synthesis of CoCr_2O_4 nanoparticles through sol-gel method.	30
Fig. 3.2: TEM.....	32
Fig. 3.3: X-Ray Diffraction.....	33
Fig. 3.4: Condition for constructive and destructive interference.....	34
Fig. 3.5: Brag's angle.....	35
Fig. 3.6: Josephson junction.....	37
Fig. 3.7: Superconducting coil in SQUID.....	38
Fig. 4.1: XRD patterns of $\text{CoCr}_2\text{O}_4/(\text{SiO}_2)_y$ nanoparticles with $y = 0\%$ and 80%	40
Fig. 4.2: TEM image of uncoated cobalt chromite nanoparticles at 100 nm scale.	41
Fig. 4.3: ZFC and FC curves for (a) uncoated cobalt chromite nanoparticles and (b) Silica coated cobalt chromite nanoparticles at different field.	43
Fig. 4.4: M-H loop of CoCr_2O_4 nanoparticles with $y = 0\%$ concentration of SiO_2 at $T = 5\text{K}$, 25K , 50K and 75K	45

Fig. 4.5: (a, b) Variation in M_s and H_c value with temperature of uncoated nanoparticles.	46
Fig. 4.6: M-H loop of $CoCr_2O_4$ nanoparticles with $y = 80\%$ concentration of SiO_2 at $T = 5K$, 15K, 25K, 50K and 75K.	47
Fig. 4.7: (a, b) Variation in M_s and H_c value with temperature of silica coated nanoparticles.	49
Fig. 4.8: (a, b) M_s Vs T and H_c vs T of Uncoated and Silica Coated Nanoparticles.	50
Fig. 4.9: (a, b) Kneller's Law fit for uncoated and 80% silica coated $CoCr_2O_4$ nanoparticles.	52

Abstract

Temperature dependent magnetic properties of uncoated and silica coated cobalt chromite (CoCr_2O_4) nanoparticles have been studied in this research work. Uncoated and 80% silica (SiO_2) coated CoCr_2O_4 nanoparticles were synthesized by using sol-gel method. The XRD analysis confirmed the normal spinel structure of CoCr_2O_4 nanoparticles. The average crystallite size was 28 nm for uncoated and 19 nm for coated nanoparticles. TEM image of CoCr_2O_4 nanoparticles showed that the nanoparticles are non-spherical in shape. SQUID magnetometer was used for studying magnetic properties. Zero field cooled/field cooled (ZFC/FC) magnetization curves of uncoated and SiO_2 coated CoCr_2O_4 nanoparticles were taken at different fields such as 50, 500 and 1000 Oe. ZFC/FC curves of uncoated CoCr_2O_4 nanoparticles underwent a ferrimagnetic transition at $T_c = 99$ K at 50 Oe, while 80% silica coated CoCr_2O_4 nanoparticles showed T_c at 95 K. Decrease in T_c was attributed to decreased surface disorder in SiO_2 coated nanoparticles. The values of T_s and T_1 for uncoated CoCr_2O_4 nanoparticles remain unchanged with increasing field due to strong spin lattice coupling, however they showed slight decrease in case of coated nanoparticles. The value of M_s for uncoated nanoparticles revealed decreasing trend with decreasing temperature due to presence of stiffed/strong conical spin spiral and lock-in states, while it showed abnormal behaviour for coated nanoparticles. The value of H_c for both uncoated and coated CoCr_2O_4 nanoparticles found increasing with decreasing temperature due to decrease in thermal fluctuations at low temperatures. The experimental H_c data was fitted by using Kneller's law and found $T_B = 75$ K, $\alpha = 0.54$ for uncoated CoCr_2O_4 nanoparticles and $T_B = 81$ K, $\alpha = 1.59$ for coated CoCr_2O_4 nanoparticles. In summary, SiO_2 coating reduced the size of nanoparticles, increased M_s below spin-spiral state ordering and decreased surface disorder in CoCr_2O_4 nanoparticles.

CHAPTER 1

INTRODUCTION

1.1 Nanoscience

Nanoscience is a rising field of science in which we investigate different properties of materials at nano scale ($1\text{nm}=10^{-9}\text{m} = 10\text{\AA}$). When we divide a bulk down to nano range, all the chemical and physical properties of the material can be changed [1]. Nanoscience is a combination of hypothetical and experimental study and includes distinctive models, laws and hypotheses.

1.1.1 Nanotechnology

The practical applications of nanoscience is nanotechnology that designs, manufactures, describes and analyzes different system, structures and devices for different applications by controlling shape and size at nano-scale. One nanometer is 10^{-9} meters. Scientists have discovered that materials at small dimensions can have significantly different properties than the same materials at larger scale [2].

1.1.2 Nano-meter Scale

“Nano” means 10^{-9} , or one-billionth part. Here it is referred to one-billionth of a meter, or 1 nanometer (nm). One nanometer is equal to 10 Angstroms. The human hair diameter is 10000 times greater than 1nm. For example when object size is 50 nm then it is 1/1000 of hair thickness and similarly one nanometer is equal to 10 hydrogen atoms, 3 gold atoms and 5 silver atoms aligned in a straight line [3]. The sizes of different objects at nano range are shown in Fig. 1.1.

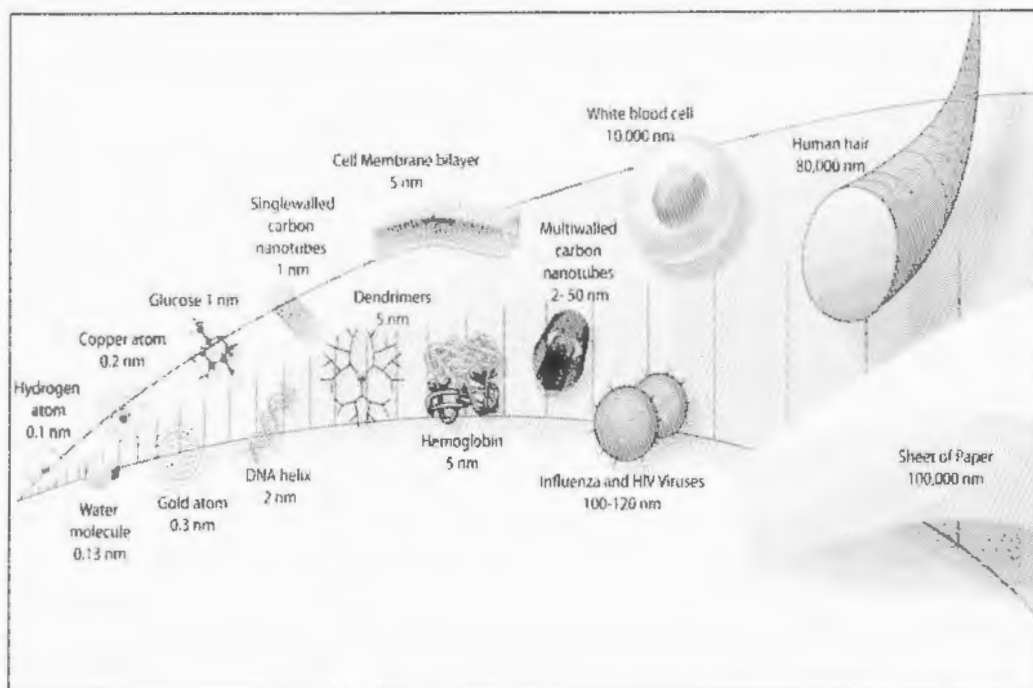


Fig. 1.1: Size of different objects at nanometre range [4].

The color of gold changes as the particle size changes at the nanometer scale. Medieval stained – glass makers were the first nanotechnologist. He knew that by putting tiny amounts of gold and silver in the glass could produce the red and yellow color in stained – glass windows. Similarly, today’s scientists and engineers have found that it takes only small amount of a nanoparticle (whether it be gold or silver), precisely placed, to change a material’s physical properties.

Gold particles in glass

Silver particles in glass

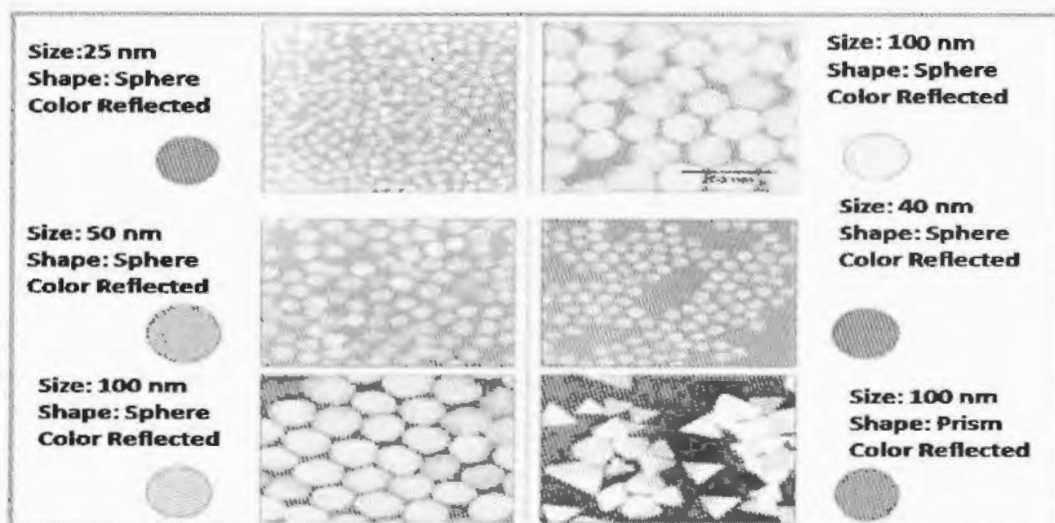


Fig. 1.2: Gold and silver particles in glass [5].

1.1.3 Unique Properties of Nanomaterials

At the nanoscale, properties of materials behave differently and governed by atomic and molecular rules. Researchers are using the unique properties of materials at this small scale to create new and exciting tools and products in all areas of science and engineering. Nanotechnology combines solid state physics, chemistry, electrical engineering, chemical engineering, biochemistry, biophysics, and materials science. It is thus a highly interdisciplinary area and involves integrating ideas and techniques from a wide array of traditional disciplines. The properties of nanomaterials or nanostructures are different from bulk material. Metals have unique properties at the nanoscale due to which some are better for conducting electricity or heat and other reflect light better or change colors. There are two reasons for changes in properties.

1. Ratio of surface area-to-volume of structure increases (most atoms are at or near the surface which make them more weakly bonded and more reactive) [6].
2. Quantum mechanical effects are important (size of structure is on same scale as the wavelengths of electrons and quantum confinement occur due to which electronic and optical properties become different). Ratio of surface area-to-volume of structure and quantum mechanical effects as shown in Fig. 1.3.

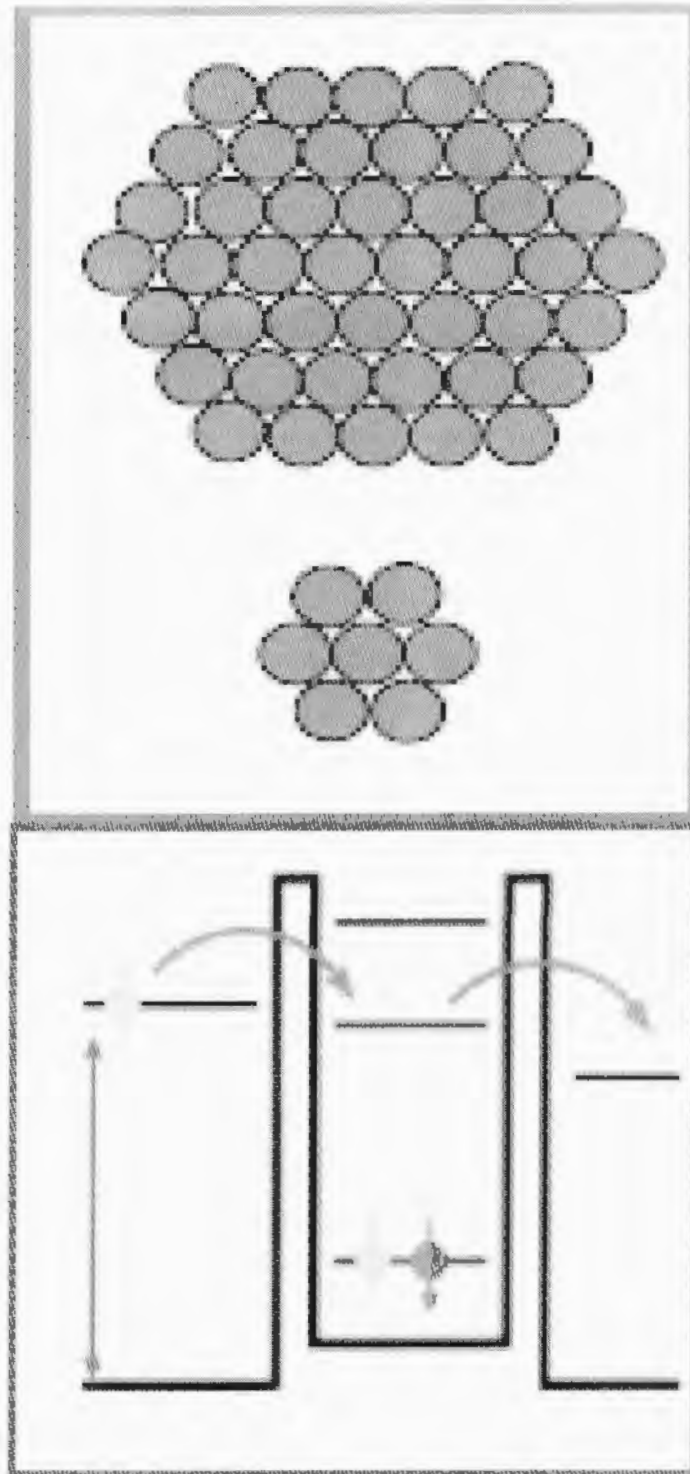


Fig. 1.3: Ratio of surface area-to-volume of structure and quantum mechanical effects [7].

1.1.4 Nanomaterials and their Classification

Nanomaterials are those materials which have at least one dimension in nanometre range. The physical, chemical, electrical, optical and thermal properties of nanomaterial are totally different from bulk material. For example conducting metals

lose their conductivity when we reduce the size from bulk to nanometre [8, 9]. The reason of change in properties of materials at nano scale is due to increase in surface area to volume ratio [6]. The nanomaterial are categorised into four types on the base of their dimensions

- 0-dimensional nanomaterial
- 1-Dimensional nanomaterial
- 2-Dimensional nanomaterial
- 3- Dimensional nanomaterial.

1.1.5 Zero-Dimensional Nanomaterials

Zero-dimensional nanomaterials are those materials which have all the three dimensions (x, y and z) in the range 1-100 nm. For example, quantum dots, nano-shells, microcapsules and hollow spheres.

1.1.6 One- Dimensional Nanomaterials

One dimensional nanomaterials are those materials which have any two dimensions in the range 1-100 nm and single-walled carbon nanotubes, fibers and nanowires are under this category.

1.1.7 Two-Dimensional Nanomaterials

Two dimensional nanomaterials are those materials which have only one dimension in the nanometer range i.e Anti-adhesive or anti-stain coatings, applied films and viruses [10]. Different type of nanomaterials are shown in Fig. 1.4.

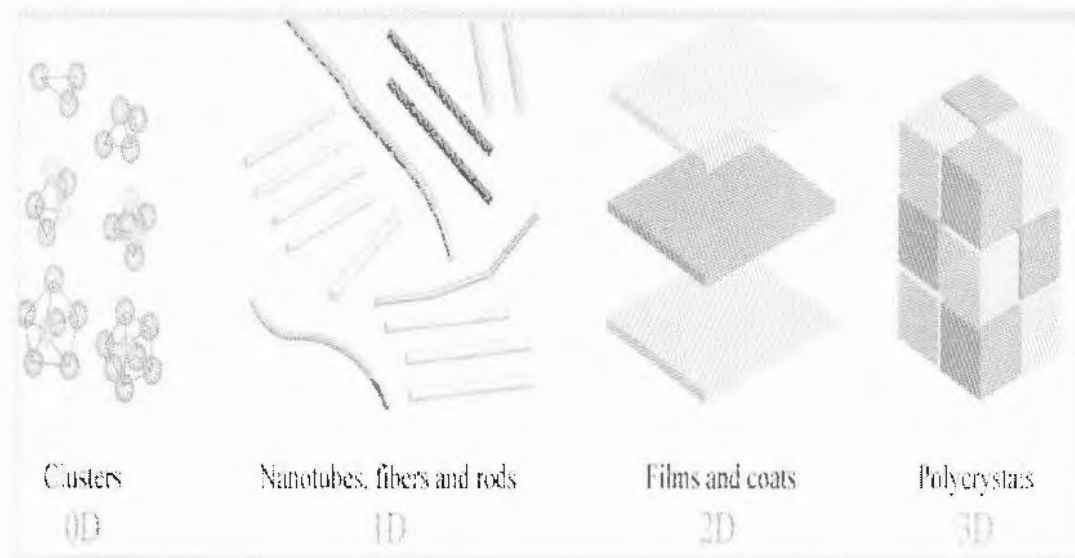


Fig. 1.4: 0- Dimensional, 1-Dimensional, 2-Dimensional and 3-Dimensional nanomaterials [11].

1.1.8 Applications of Nanomaterials

Nanoscience is an interdisciplinary field which involves physics, chemistry, material science and biology. It has wide range of applications in different fields at global level. Nano materials are used in many technological fields such as food, gas sensor, sports goods, medical, optical and electrical [12]. There are various applications of nanoparticles in different fields. Some are listed below:

- **Aerospace:** Landing things coatings, thrusters and body materials.
- **Automotive:** Attrition safe coatings and start plugs.
- **Consumers:** Wear gear, TVs, hand held gadgets makeup and PCs.
- **Environmental:** Water maintenance, contamination control and fired layers.
- **Industrial Coatings:** Natural coatings (Chromium, Cadmium and Beryllium).
- **Medical:** Embed coatings, antimicrobials coatings, sensors and remedial medications.
- **Powers:** Controlled transformers, sun oriented boards
Fuel Cells (Microbial power modules).

Nanotechnology has various applications in our many practical fields of life. Some useful applications of nanotechnology are described below in Fig. 1.5.

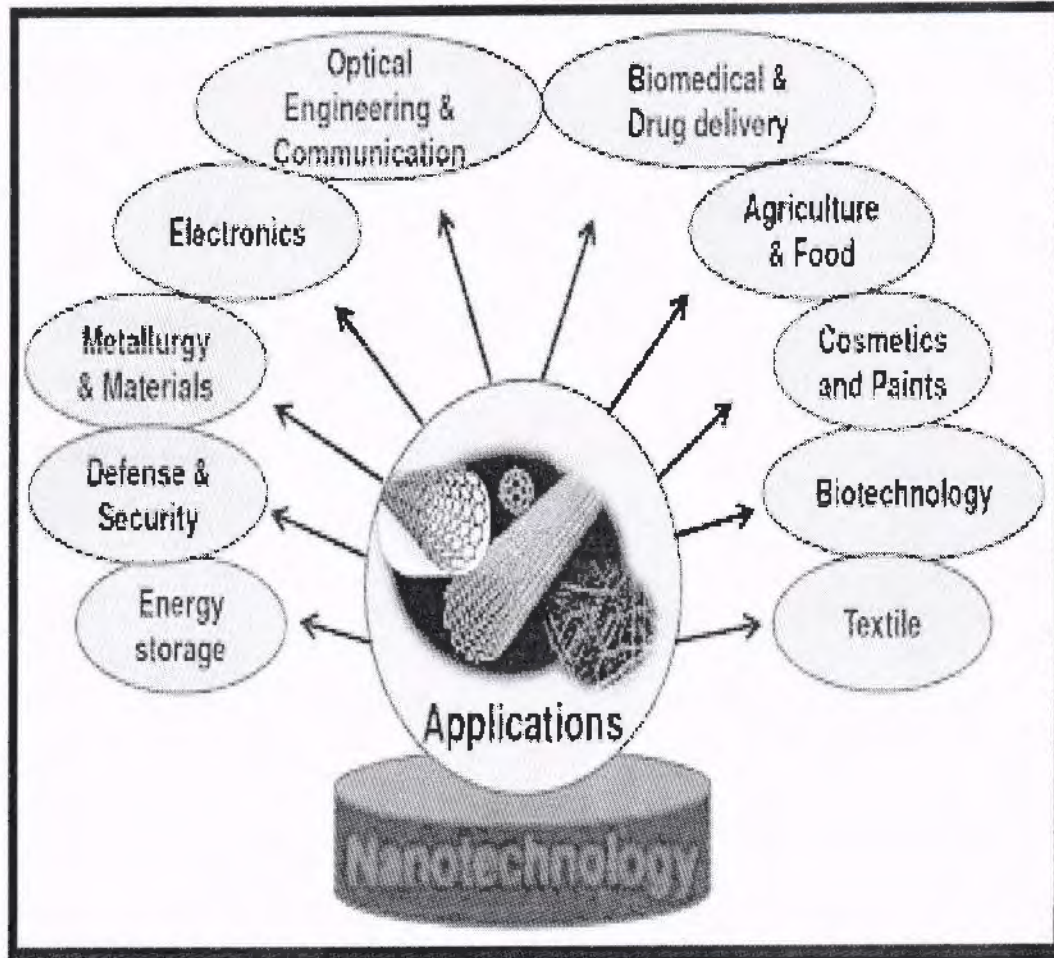


Fig. 1.5: Practical applications of nanotechnology [13].

1.2 Magnetism

The phenomenon in which material shows certain type of reaction such as attraction or repulsion under the effect of an applied external magnetic field is called magnetism [14]. About 250 years earlier, near the city magnesia phenomenon of magnetism was first time observed on the piece of iron. Phenomenon of magnetism can be observed in computers, devices which store data, electric motors, transformers and many more. The ratio between magnetic dipole moment and volume is called magnetization (M) [15] and we write it mathematically as

$$M = m/v \quad (1.1)$$

Where, “ v ” is the volume, “ m ” is magnetic dipole moment and M is the magnetization with unit A/m [16].

The above equation 1.9 shows that “B” is directly proportional to “H” [14].

1.2.1 Origin of Magnetism

Electron possesses two types of motion, first is orbital motion and second is the spin motion. Spin and orbital motion is the source of magnetism in materials. If the magnetic moment due to the orbital motion of electron in an atom around the nucleus and due to the spin motion is same then material shows strong magnetic behaviour because both moments contribute to the total magnetic moment of the material. Gold, nickel, cobalt and many other are the examples of the magnetic material [17]. The orbital and spin moment of electron is shown in Fig.1.6.

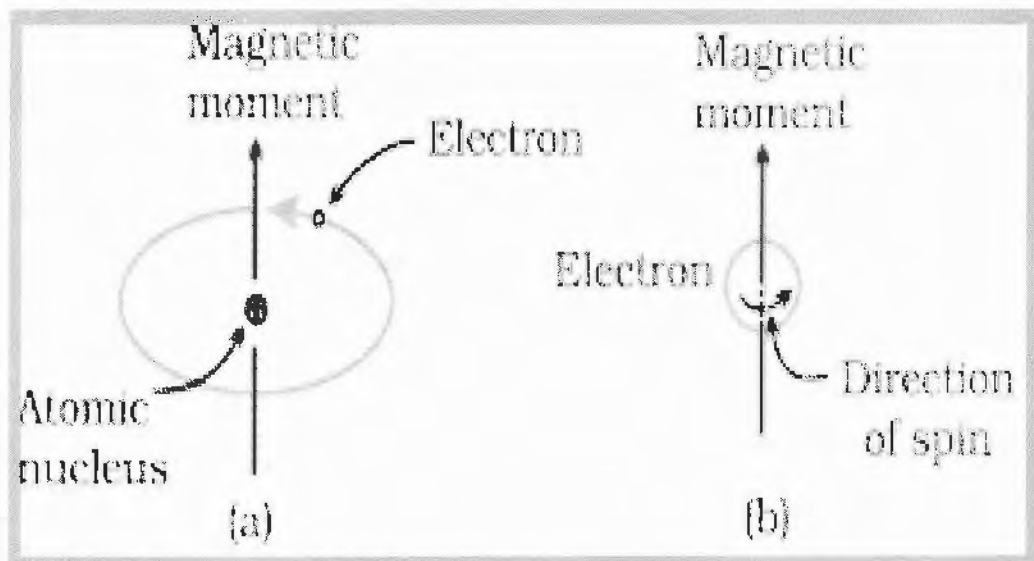


Fig. 1.6: Spin and orbital motion of electron in an atom [18].

1.2.2 Magnetism by Nucleus

Both neutrons and protons present inside the nucleus and they also have magnetic moments. Magnetic field produced by nucleus is very weak due to their heavier masses and we can neglect their magnetic fields.

1.3 Classification of magnetic material

When different types of magnetic materials are placed in external magnetic field they behave differently. We divide different magnetic materials into five types which are listed below

- Diamagnetic materials
- Paramagnetic materials
- Ferromagnetic materials
- Anti-ferromagnetic materials
- Ferromagnetic materials [19]

Periodic table in Fig. 1.7 shows different magnetic materials according to their classification.

1												2						
1	2											3	4					
H	He																	
3	4											5	6	7	8	9	10	
Li	Be											B	C	N	O	F	Ne	
11	12											13	14	15	16	17	18	
Na	Mg											Al	Si	P	S	Cl	Ar	
19	20	21	22	23	24	25	26	27	28	29	30	31	32	33	34	35	36	
K	Ca	Sc	Ti	V	Cr	Mn	Fe	Co	Ni	Cu	Zn	Ga	Ge	As	Se	Br	Kr	
37	38	39	40	41	42	43	44	45	46	47	48	49	50	51	52	53	54	
Rb	Sr	Y	Zr	Nb	Mo	Tc	Ru	Rh	Pd	Ag	Cd	In	Sn	Sb	Te	I	Xe	
55	56	57	72	73	74	75	76	77	78	79	80	81	82	83	84	85	86	
Cs	Ba	La	Hf	Ta	W	Re	Os	Ir	Pt	Au	Hg	Tl	Pb	Bi	Po	At	Rn	
87	88	89																
Fr	Ra	Ac																
			58	59	60	61	62	63	64	65	66	67	68	69	70	71		
			Ce	Pr	Nd	Pm	Sm	Eu	Gd	Tb	Dy	Ho	Er	Tm	Yb	Lu		

Fig. 1.7: Magnetic behaviour of material [20].

1.3.1 Diamagnetism

Under the application of external magnetic field if the magnetic moments align themselves in opposite direction to the external magnetic field then this phenomena is referred as diamagnetism. And the materials which show this phenomenon are called diamagnetic material. Michael Faraday introduced the diamagnetic behaviour of material in 1847. He saw some repulsion when he placed the sample of bismuth near the heavy duty magnet. If external magnetic field is not applied across this type of material the magnetic moments due to orbital and spinning motion of electrons in an atom are cancel out and net magnetic moment is zero. If the external magnetic field is applied across the diamagnetic materials, they align in opposite direction to the applied magnetic field. Examples of diamagnetic materials

are silver, copper and gold [17]. Behaviour of diamagnetic material with and without applied magnetic field is shown in Fig. 1.8.

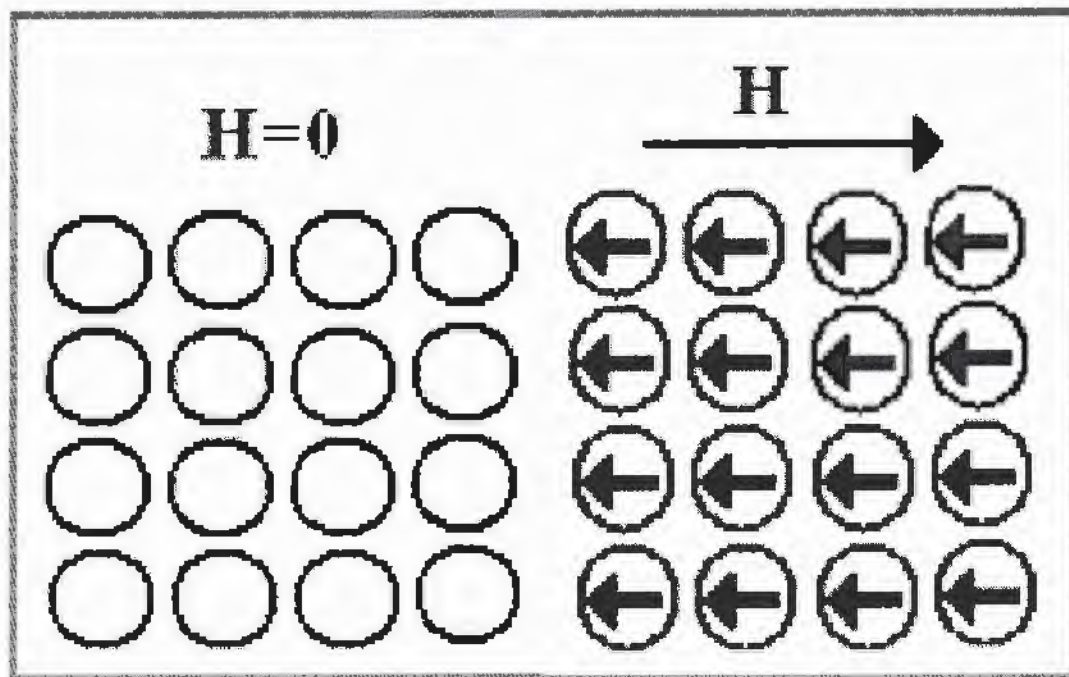


Fig. 1.8: Diamagnetic material in presence of field and zero field [21].

The magnetic susceptibility of diamagnetic material is less than zero i.e. ($\chi_m < 0$). According to Lenz's law, the applied field is opposed by the induced magnetic field so diamagnetic susceptibility is field dependent. The effect of temperature and applied magnetic field on magnetic susceptibility in diamagnetic material is as shown in Fig. 1.9.

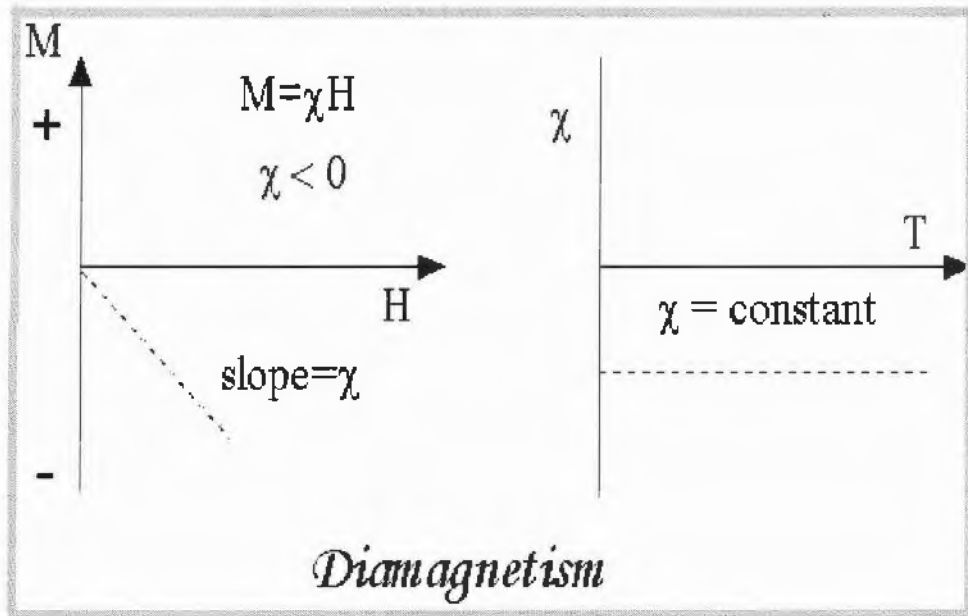


Fig. 1.9: Diamagnetic material behaviour with temperature and magnetic field [22].

1.3.2 Paramagnetism

Under the application of external magnetic field if the magnetic moments align themselves parallel to the direction of applied field this phenomenon referred as paramagnetism and material which show this phenomenon is called paramagnetic material. Initially when the magnetic field is not applied to the material, orientation of magnetic moments is random and the resultant magnetization is zero because the magnetic moments are randomly aligned. Under the application of magnetic field total magnetization of the material is not zero because magnetic moments are aligned in one particular direction which is parallel to the applied magnetic field. This alignment of the magnetic moments depends upon the strength of external applied magnetic field [23]. Pt, Al and Cr are examples of paramagnetic materials. Fig. 1.10 shows the behaviour of paramagnetic material with and without applied magnetic field.

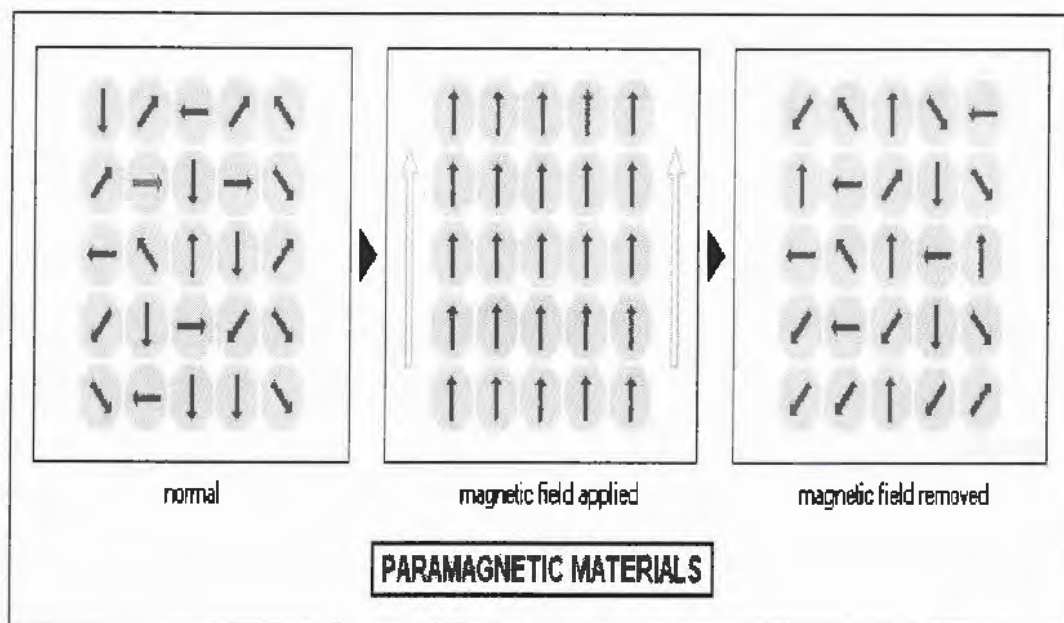


Fig. 1.10: Behaviour of paramagnetic material with and without applied magnetic field. [24].

The susceptibility of paramagnetic material is positive and its value is very small on the other side it has inverse relationship with temperature, when temperature increases the susceptibility decreases as shown in Fig. 1.11 [25].

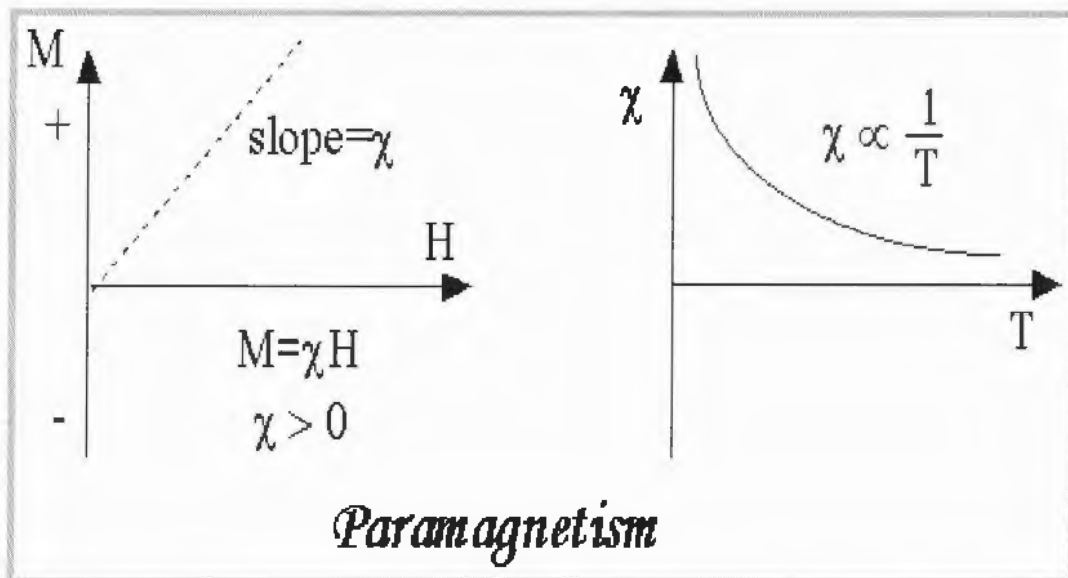


Fig. 1.11: Paramagnetic material behaviour with temperature and magnetic field [26]

1.3.3 Ferromagnetism

Ferromagnetism is exhibited by those materials that possess unpaired electrons and spontaneous magnetisation. In ferromagnetic materials atoms are so close to each

other that their wave functions overlap and this is the property which make them different from paramagnetic one. Ferromagnetic materials contain small regions in which all magnetic moments are unidirectional and these regions are named as domain as shown in Fig. 1.12 (a) and (b). The size of these magnetic domains ranges from few microns to about 1 mm. In these magnetic domains, every domain contains about 10^{12} to 10^{16} atoms. The transition region between domain and its neighbouring about 100 atoms is called domain walls.

In the absence of applied external magnetic field the magnetic moments are unidirectional in a single domain while magnetic moments in different domains possess different direction. In the presence of external applied magnetic field the walls of the magnetic domains arrange themselves in the direction of applied magnetic field.

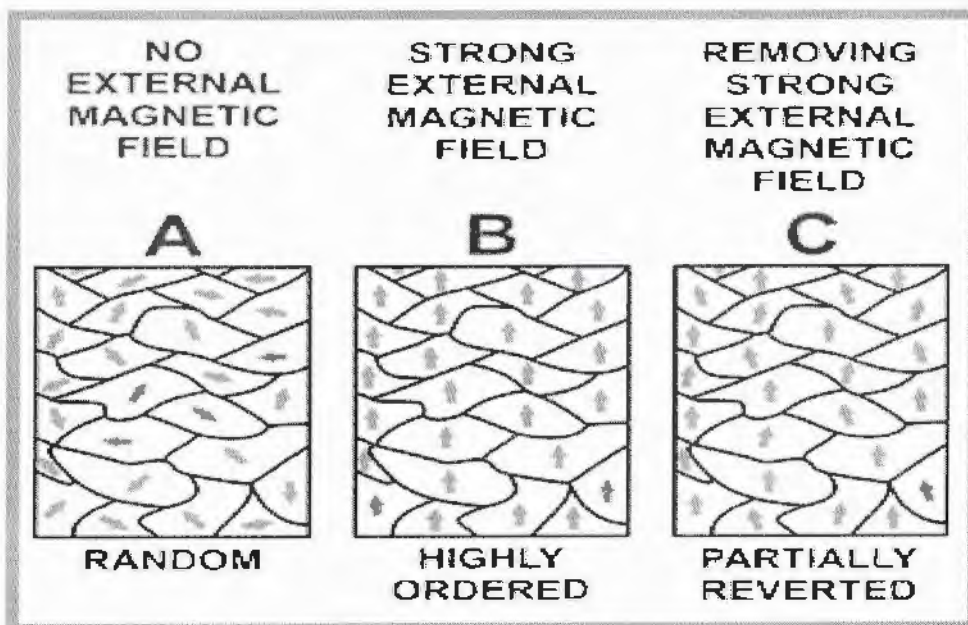


Fig. 1.12: Ferromagnetism behaviour (a) in the absence of magnetic field (b) when magnetic field is applied [27].

1.3.4 Anti-ferromagnetism

Antiferromagnetic materials contain magnetic moments which are aligned in anti-parallel fashion when no external magnetic field is applied and in this condition net magnetization is zero $M=0$. In these magnetic materials, the magnetic moments are equal in magnitude but in opposite direction and cancel the effect of each other.

Examples of Anti-ferromagnetic materials are FeTiO_2 , MnO and FeS . Cr is the only element in the periodic table which is anti-ferromagnetic material [14, 17]. The order of the magnetic moments in anti-ferromagnetic material is shown in Fig. 1.13.

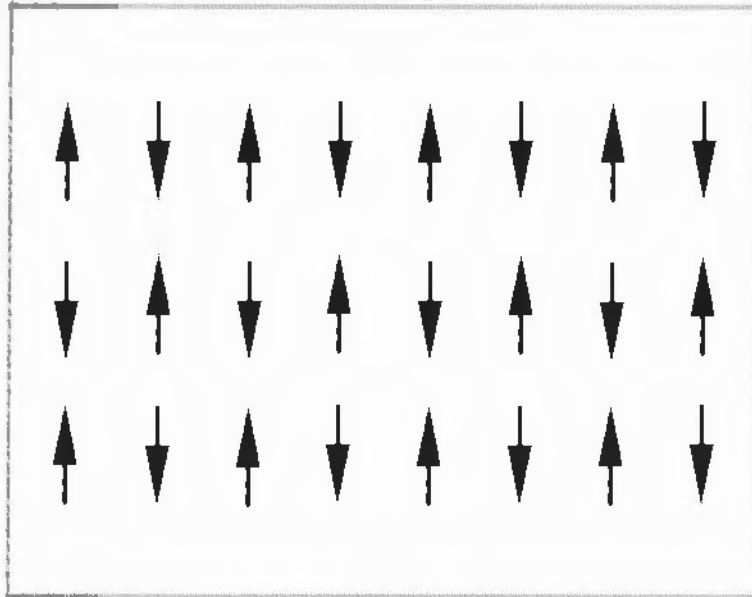


Fig. 1.13: order of magnetic moments in anti-ferromagnetic materials [28].

Anti-parallel arrangement of magnetic moments is maintained at very low temperature while at Neel temperature or high temperature magnetic moments of atoms are misaligned and becomes paramagnetic.

1.3.5 Ferrimagnetism

In ferrimagnetic materials, under the absence of applied magnetic field the magnetic moments are anti-parallel and have unequal magnitude. Domains exist in ferrimagnetic materials like anti-ferromagnetic and ferromagnetic materials [14, 17]. Example of ferrimagnetic material is magnetite. Opposite and unequal alignment of magnetic moments in the ferrimagnetic materials is shown in Fig. 1.14.

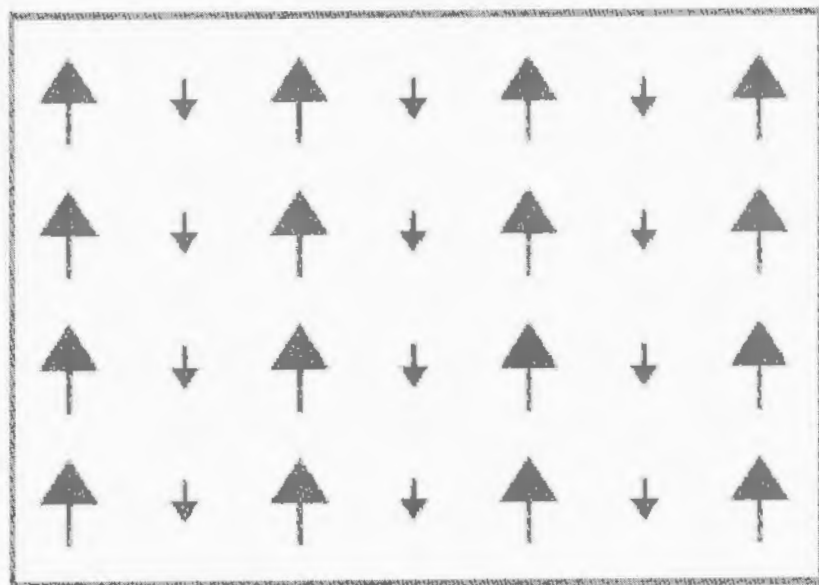


Fig. 1.14: Anti-parallel alignment of ferrimagnetism [29].

1.4 Superparamagnetism

Superparamagnetism is a fact that arises in a single domain magnetic material. These materials show a strong interior magnetization due to the exchange coupling of electrons when located in external magnetic field. They have moderate level of induced magnetization. They have magnetic susceptibility in between paramagnetic and ferromagnetic. These materials have zero coercivity [30-33]. When the size of CoCr_2O_4 reduces down to 5nm, it shows superparamagnetic behaviour [34, 35]. In superparamagnetic material, thermal energy is greater than anisotropy energy and mathematically anisotropic energy is given as

$$E_A = KV\sin^2\theta \quad (1.10)$$

Where V , K and θ are volume of particle, magnetic anisotropic constant and angle between easy axis and magnetization, respectively.

1.4.1 Blocking Temperature

Temperature at which we get maximum value of magnetization while taking zero cooled field curve (ZFC) is referred as blocking temperature (T_B). When spin flip time is greater than measurement time $\tau_0 > \tau$, system is in blocked state so particle exhibits higher value of coercivity and when the spin flip time is less than

measurement time $\tau_0 < \tau$, system is in unblocked state so particle demonstrates lower value of coercivity. The transition between blocked and superparamagnetism state happens when $\tau_0 = \tau$. So the temperature at which $\tau_0 = \tau$ is called Blocking temperature [36].

1.4.2 Neel Theory

The mechanism to overcome the flipping time and anisotropic energy is described by Neel in 1947 whose mathematical equation is:

$$\tau = \tau_0 \exp (E_A/K_B T) \quad (1.11)$$

Where τ_0 and τ are the spin flip time and measurement time, respectively [37]. The calculated value of τ_0 from Neel ranges from 10^{-9} to 10^{-10} [38]. The above equation describes that if $\tau > \tau_0$ the nanoparticles will be in superparamagnetic state and if $\tau < \tau_0$ then nanoparticles are in block state [39-42].

1.4.3 Curie Temperature

The temperature at which material changes from ferromagnetic material to paramagnetic material is called Curie temperature. At Curie temperature saturation magnetization of material vanishes. According to Curie-Weiss law [43].

$$\chi = C/(T - T_C) \quad (1.12)$$

Where T_C is Curie temperature, "C" is Curie constant and χ is known as magnetic susceptibility. Magnetic moments in a domain keep them align in a parallel fashion below the Curie temperature and interactions between them are strong. If temperature rises to Curie temperature, thermal energy becomes sufficient to remove coupling energy as a result more and more magnetic domains are randomly aligned and material changes from ferromagnetic to paramagnetic [44] as shown in Fig. 1.15.

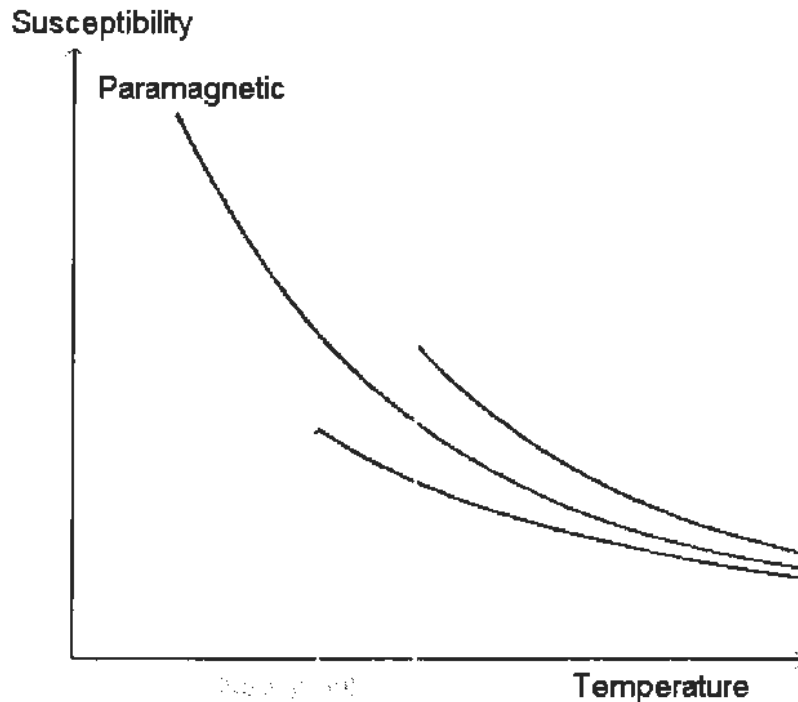


Fig. 1.15: Temperature effect on magnetic material [45].

1.5 Hysteresis

A phenomenon which takes place when there is magnetization and demagnetization of medium. Fig. 1.16 shows a coil which is attached with a source of current. When switch is on current flows through the coil and magnetic field is produced in that coil and nature of magnetic field will depend upon the nature of current. When an iron cylinder placed in the coil the magnetic field is also produced in the cylinder due to external magnetic field. The external magnetic field is called magnetizing field (H) and magnetic field that is produced in the cylinder due to external magnetic field, is called magnetic field (B) as shown in Fig. 1.16.

In ferromagnetic material, domains are present in the form of close circuit every North Pole attach with South Pole and vice versa and $B = 0$ when no external field applied.

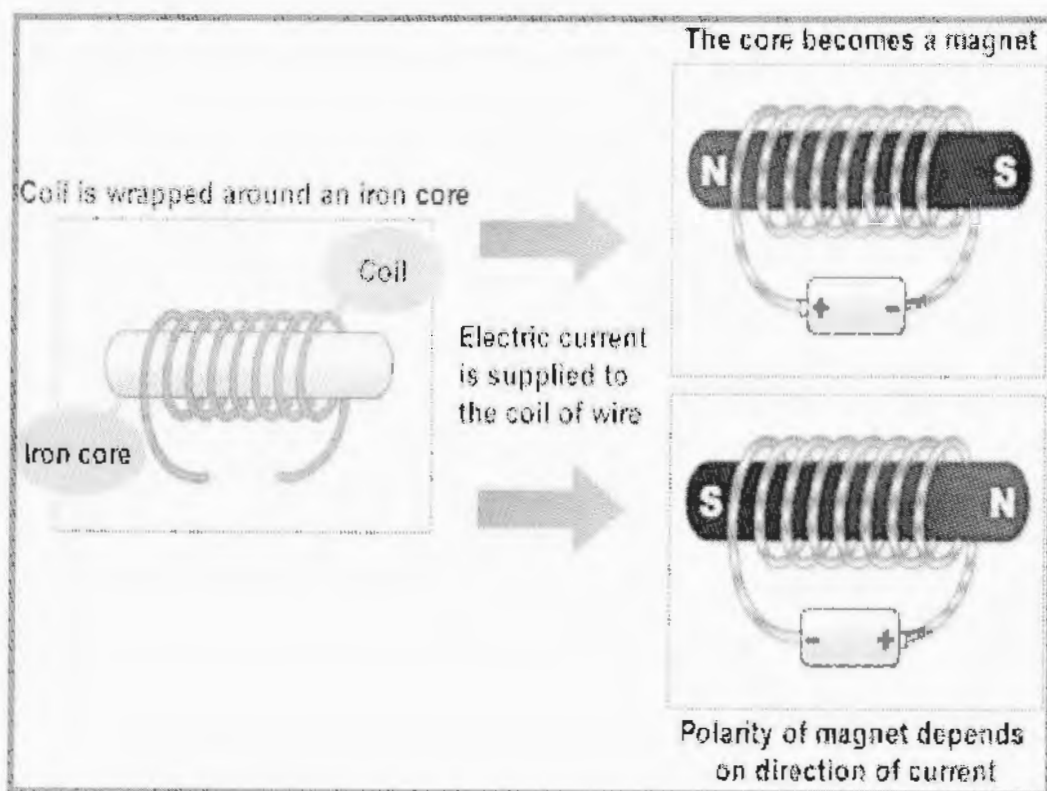


Fig. 1.16: Flow of current through coil [46].

When we increase the external field (H), magnetic field (B) increases and reaches at a point where we further increase H but B does not increase because all the magnetic domains are aligned in the direction of external magnetic field and this point is known as saturated point. Now we decrease the value of H the value of B also decreases because all magnetic domains are again aligned randomly with decreasing field. When H is zero but B is not zero because some domains are still aligned and as a result some magnetization will also present in material and this is called remanence. Now we increase H in negative direction the remaining magnetization will finish. Further, we increase the H in negative direction the magnetic domains are also aligned in opposite direction and again at a point magnetization are saturated and again we decrease H up to zero and then increase until B shows saturation and formed hysteresis loop as shown in Fig. 1.17.

1.5.1 Saturation Magnetization

External magnetic field forces the magnetic domains to align in the direction of external magnetic field. A stage comes when material shows maximum magnetization and no further magnetization takes place. This maximum value of

magnetization is called saturation magnetization [47]. It is denoted by M_s as shown in Fig. 1.17.

1.5.2 Remanent Magnetization

When the external magnetic field is reduced the magnetization, B is also reduced but at 0 Oe material shows some magnetization and it is symbolized as "ob" in Fig. 1.17. This magnetization is called remanent magnetization and it is denoted by M_r .

1.5.3 Coercivity

Coercivity is that value of H which is required to make residual magnetization zero, is called coercivity which is symbolized by "oc" in Fig. 1.17.

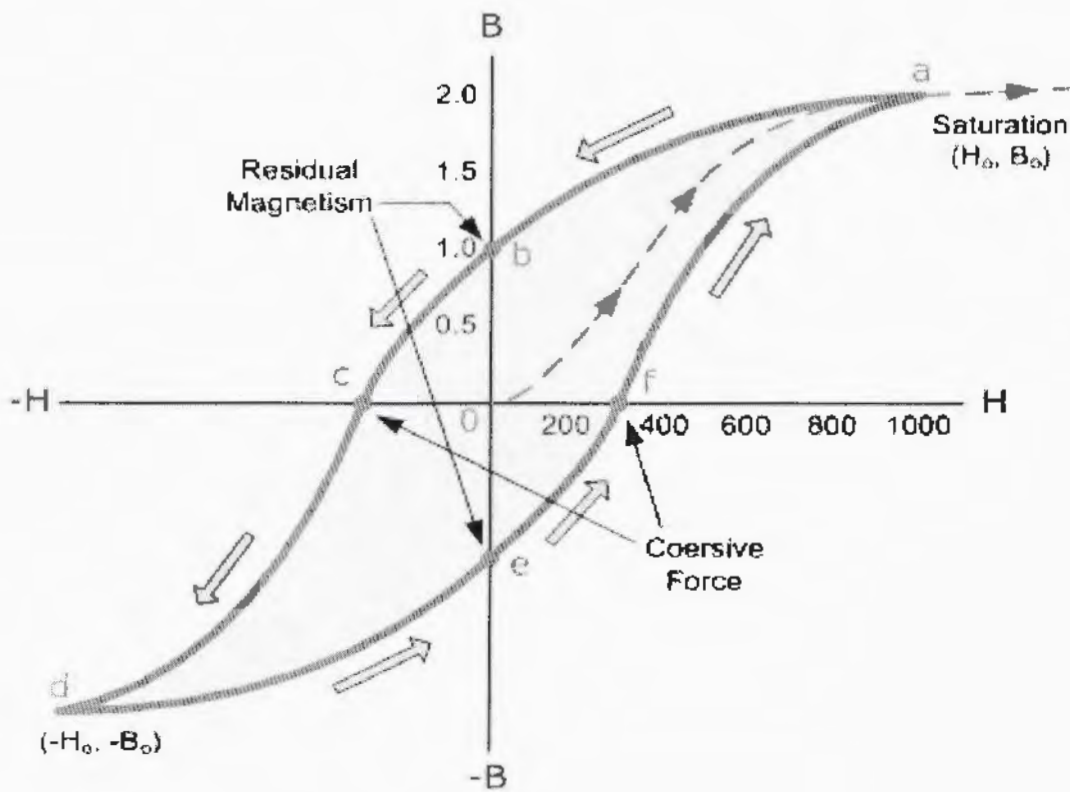


Fig.1.17: Hysteresis loop of ferromagnetic material [46]

1.6 Chromites

Chromites are spinel ferrimagnetic compounds which contain chromium ion as a necessary element. The general formula of chromites is $A^{2+} Cr^{3+}_2 O^{2-}_4$. Where

divalent ions are occupied at A site and trivalent ions are occupied at B site which is Cr. CoCr_2O_4 , ZnCr_2O_4 and NiCr_2O_4 are most prominent examples of chromites.

1.6.1 Structure of Chromites

Structure of chromites is FCC cubic spinel. The structure of spinel compounds is closed pack and unit cell is made by 32 oxygen atoms. The ions reside on two sites e.g. A which is tetrahedral site and B which is octahedral site in this configuration. Tetrahedral site A surrounded by four atoms of oxygen while octahedral site B surrounded by six atoms of oxygen.

Total tetrahedral sites are 64 and octahedral sites are 32 those are available in the spinel cubic structure. Total 8 tetrahedral and 16 octahedral sites are filled out of 64 and 32 tetrahedral and octahedral sites [48].

In spinel structure octahedral and tetrahedral sites are indicated in Fig. 1.18.

Spinel AB_2O_4

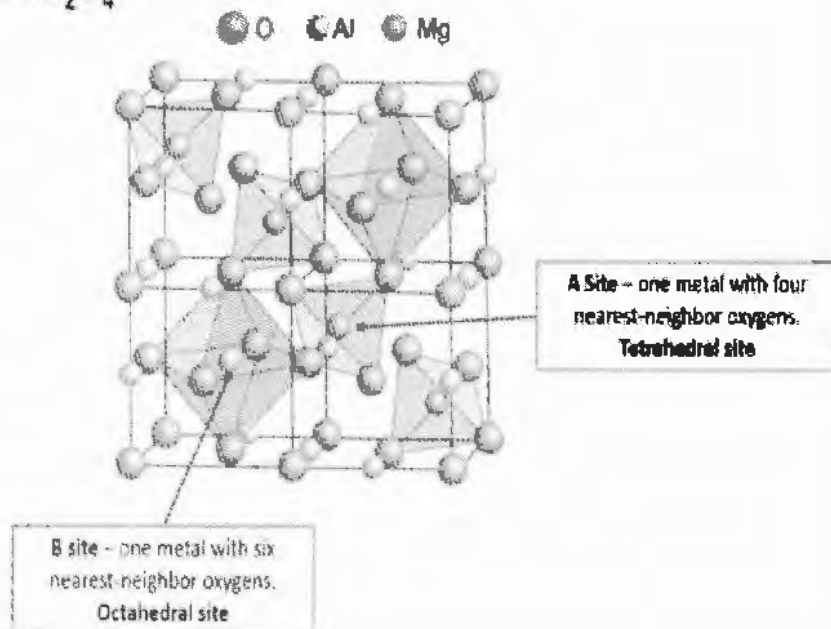


Fig.1.18: Crystal Structure of Spinel Chromite [49].

1.6.2 Cobalt Chromite (CoCr_2O_4)

Cobalt chromite (CoCr_2O_4) is a multiferroic material having several application in various field such as data storage, communication system, sensor, ferro

fluid, random access memory and many more [50, 51]. Multiferroic possess both electric and magnetic properties [52].

1.6.3 Effect of SiO₂ surface coating

Magnetic and other properties of nanoparticles are size dependent [53, 54]. Amorphous silica possess some unique properties as compare to other non-magnetic material such as Al₂O₄ and TiO₂ [55]. The SiO₂ surface coating can control the particle size, interacts with the surface spins, reduces the agglomeration, controls the surface anisotropy and controls the magnetic transitions [56].

CHAPTER 2

LITERATURE REVIEW

2.1 Literature Review

Nadeem *et al.* [57] studied the effect of different concentration of silica (SiO_2) (10%, 30%, 50% and 60%) on dielectric, magnetic and structural properties of $\text{CoFe}_2\text{O}_4/\text{SiO}_2$ nanoparticles. Nanoparticles of $\text{CoFe}_2\text{O}_4/\text{SiO}_2$ are prepared by sol-gel method. X-ray diffraction is use for all samples to study the structure of material. It is observed that when the concentration of SiO_2 is increased, the average size of crystal is decreased due to the formation of nucleation sites. The growth of nanoparticles is well controlled by SiO_2 matrix. Spinel ferrite's formation was confirmed by Fourier transform infrared spectroscopy. Scanning electron microscopy image shows that particles are spherical and less agglomerate. It is studied that when the concentration of SiO_2 is increased, size of particle as well as magnetization decreased. Magnetization of larger nanoparticles is high as compare to small nanoparticles because of surface spin disordered. It is observed that all dielectric parameters depend on the concentration of SiO_2 . Reduction in dielectric and magnetic properties depend upon the crystallite size with increasing the concentration of SiO_2 . Therefore, in ferrite nanoparticles concentration of SiO_2 is use to control the magnetic properties, size of nanoparticles and dielectric properties.

Nadeem *et al.* [56] studied the influence of different concentration ($x = 0\%$, 15%, 30%, 45% and 60%) of silica (SiO_2) on magnetic, structural and dielectric properties of maghemite nanoparticles. Cubic inverse spinel structure of nanoparticles having concentration $x = 0\%$, 15% and 30% was confirmed by XRD. When the concentration of SiO_2 increased both lattice constant and average crystallite size were decreased. Self-organized leaf like shape and spherical shape of nanoparticles can be observed in the SEM image. Tangent loss and dielectric constant are the parameters which are decreased when frequency increased and at higher frequency they were constant. Value of AC conductivity is higher at higher frequency. In conclusion the

surface coating of SiO_2 can be used to control the size of nanoparticles and change the dielectric and magnetic properties of maghemite nanoparticles.

Nadeem *et al.* [58] synthesized the NiFe_2O_4 nanoparticles dispersed in SiO_2 by sol-gel method. Usually sol-gel method provides multiphase nanocomposites. It is studied by using different techniques that how a single phase structure can be obtain from a multi-phase composite, when it is annealed at different temperature. The average size of particle lies between 16-27 nm ranges. Chemical phases are NiFe , NiO , Fe_2O_3 , and NiFe_2O_4 formed below 900°C .

Nogues *et al.* [59] observed the phenomenon of exchange bias FM (ferromagnetic) and AFM (anti-ferromagnetic) composite nanoparticles. The presence of exchange bias (EB) is confirmed by hysteresis loop shift. Below the Neel temperature the coercivity H_c of nanostructure is increased after the field cooling procedure. When temperature is increased, and reached at AFM T_N , effect of exchange bias is disappeared. Temperature where exchange bias effect is zero is known as blocking temperature. Exchange bias is also depending upon the size of nanoparticles.

Moran *et al.* [60] studied the exchange bias phenomenon and its related effects on AFM- FM structure. It is studied that when FM material and AFM material interfaces is cooled, exchange bias is produced in FM. Exchange bias is the phenomenon connected with anisotropy, formed at interface b/w FM and AFM material. Bean and Meikle-john discovered anisotropy during study. Interface coupling is observed while cooling the FM- AFM couple and magnetic field is applied above the Neel temperature and below the curie temperature ($T_N < T < T_C$) to $T < T_N$. FM-AFM hysteresis loop shift along fixed axis is usually observed negative or opposite direction of cooling field at $T < T_N$. Coercive field value is different for increasing and decreasing the field and this loop shift is called exchange bias H_E . After field cool process coercivity H_C is increased.

Kanran *et al.* [61] studied the effect of different concentrations of SiO_2 on the magnetic properties and structure of multiferroic CoCr_2O_4 nanoparticles. By using sol-gel method nanoparticles of CoCr_2O_4 are prepared having crystallite size ranging from 19nm to 28nm. It was studied that when the concentration of SiO_2 is increased, the cell parameter and average size of crystal is decreased. ZFC and FC measurements were also done. Nanoparticles of materials suffered from paramagnetic state to ferromagnetic short range state. when the size of crystal is decreased or when

concentration of SiO_2 is increased then transition temperature PM-FM have been decreased from 101 K to 95 K. Conical spin state for all the sample is observed for all the samples which also decreased when size of crystal is decreased. Saturation magnetization (M_s) also depends upon size of the crystal and decreased when concentration of SiO_2 is increased because average crystal size decreased. AC susceptibility showed transition temperature decrease, T_c peak broadening, magnetization decreased when SiO_2 concentration increase.

Kamran *et al.* [62] studied the magnetic, dielectric and structural properties of $\text{Co}_{1-x}\text{Mg}_x\text{Cr}_2\text{O}_4$ nanoparticles with concentration ($x = 0, 0.2, 0.4, 0.6, 0.8, \text{ and } 1$) of Mg prepared by sol-gel method. XRD showed $[\text{A}]_{\text{tet}} [\text{B}_2]_{\text{oct}} \text{O}_4$ (normal spinel structure) of both MgCr_2O_4 and CoCr_2O_4 . Both Mg^{2+} and Co^{2+} occupied by tetrahedral site and Cr^{3+} occupied by octahedral site and did not observed extra impurities peaks. The average size of crystal displayed non-monotonic peak behaviour with $x = 0.6$ concentration of Mg. The $\text{Co}_{1-x}\text{Mg}_x\text{Cr}_2\text{O}_4$ single phase normal spinel nanoparticles were confirmed by FTIR and Raman. ZFC/FC curved opened at T_c by magnetic transition when material change from PM to FM and at T_s the state is spiral spin. When the concentration of Mg increased both T_s and T_c decreased and finally at T_N with $x = 1$ concentration of Mg system goes to AFM. And improve the dielectric properties for nanoparticles with $x = 0.6$ concentration of Mg.

Stamps *et al.* [63] studied that exchange bias is a very important and a very interesting problem which discuss some basic issues of magnetism and includes exchange bias interactions, impurity and disorder effect at interface. There are two types of exchange bias one in which partial walls are reversible, and the other in which asymmetric hysteresis loops are form due to irreversible process. Partial wall by reversible bias cannot loss completely when asymmetric hysteresis is form. Exchange bias also depend upon the temperature. Mean field was calculated, shows that exchange bias and coercive field both are decrease when temperature is increase.

Joshi *et al.* [64] prepared the nanoparticles of NiFe_2O_4 by using the co-precipitation method. The optical properties and magnetic properties of NiFe_2O_4 nanoparticles were explored by using Raman spectroscopy, XRD and dielectric measurements. The single spinel crystal structure of NiFe_2O_4 nanoparticles confirmed from XRD pattern and average crystallite size NiFe_2O_4 nanoparticles found in 8-20 nm range by using Debye-Scherrer's formula. The combined spinel structure of nanoparticles was proved by Raman spectroscopy. Dielectric values of nanoparticles

were strongly dependent upon temperature at all frequencies. Ac conductivity recommends that the transmission in nanoparticles is because of weak polaron vaulting among $\text{Fe}^{3+}/\text{Fe}^{2+}$ particles.

Atif *et al.* [65] synthesised the nanoparticles of zinc doped nickel ferrite by using sol-gel method. The structure of these nanoparticles was cubical spinel structure which was confirmed by X-ray diffraction pattern. Magnetic properties of these nanoparticles were studied by using super magnetic quantum interference device (SQUID) magnetometer. Saturation magnetization of these nanoparticles increased with exchange of Zn^{2+} up to certain level and after that its value becomes decreased. Dielectric measurements of these nanoparticles were done at room temperature. Initially it can be seen that ac conductivity, tangent loss decreased and when Zn^{2+} ions substituted up to certain level, increasing trend was observed. Dielectric parameters of these nanoparticles were explained by using electron vaulting mechanism.

Martinez *et al.* [66] studied that the nanoparticles of $\gamma\text{-Fe}_2\text{O}_3$ having high surface to volume ratio and show both magnetic effect and exchange anisotropy. The processes field cooled –zero field cooled (FC-ZFC) and strong field irreversibility MH curves also detected at the same time. At $T_F \approx 42$ K low temperature spin-glass behaviour is verified with high irreversibility even $H = 55$ kOe. $T_F(H)$ changes following well-known de Almeida–Thouless line $\delta T_F = H^{2/3}$. The exchange anisotropy H_E of thermal dependence is described by random field model. From this framework, he determined the surface spin glass of 0.6 nm thick layer.

Eftaxias *et al.* [67] studied that the coercive field of fused magnetic nanoparticles with core or shell morphology and effect of antiferromagnetic shell on exchange bias by using technique Monte Carlo simulation. He also studied that the coercive field is largely depend on interface size, while the exchange bias field mostly depend on interface structure and less depend on its size. When the thickness of core of given particle size is reduced and as a result both coercive field and exchange bias field are increased. He also studied that the coercive field is reduced and exchange bias field is increased when the thickness of shell increased. It was investigated that the coercive field is reduced and exchange bias field is increased when the strength of interface and shell exchange coupling increased. At the end, it was found that results of exchange bias field depend strongly on temperature than coercive field.

CHAPTER 3

SYNTHESIS AND CHARACTERIZATION TECHNIQUES

3.1 Fabrication Techniques of Nanomaterial

There are two approaches or techniques for the synthesis of nanomaterial or nanoparticles.

1. Top down approach
2. Bottom up approach

3.1.1 Top Down Approach

In this technique or approach we divide or break the bulk material down to atomic level for fabrication of nanoparticles [68]. There are many methods for the fabrication of nanoparticles by using top down approach such as:

- Ball milling method
- Laser ablation method
- Lithography

Some difficulties are present in this technique

- Significant damage of crystallographic arrangement
- Defectiveness of surface structure
- Broad size dispersal.

3.1.2 Bottom Up Approach

In this technique or approach we form nanoparticles by collecting atom by atom, molecules by molecules and cluster by cluster [69]. This approach is very beneficial approach as compare to Top down approach because it is

- Easy to control
- It is reproducible method
- Structural analysis is easy

- Particle shape and size easily controlled
- Morphology optimization
- Homogeneous chemical composition
- Cheap
- High degree of crystallinity.

Some advantages while using this process are:

- 1) Nano structure with reduced number of defects are obtained
- 2) Homogeneous chemical composition of nano structure
- 3) Long range order nanostructure is formed.

There are some different techniques which are included in bottom up approach are given bellow:

- Physical Vapour deposition
- Electrochemical deposition
- Hydrothermal technique
- Chemical Vapour Deposition
- Sol-gel method
- Co-precipitation method
- Precursor method.

3.2 Synthesis of $\text{CoCr}_2\text{O}_4/\text{SiO}_2$ Nanoparticles

There are many methods for the fabrication of nanoparticles but I chose sol-gel technique for fabrication of $\text{CoCr}_2\text{O}_4/\text{SiO}_2$ nanoparticles because of some basic reasons which are given bellow:

- Uniform distribution of particle size
- Non-destructive technique
- Homogenous formation
- Low cost method.

We have used following precursors in a stoichiometric ratio:

- Cobalt nitrate ($\text{Co}(\text{NO}_3)_2 \cdot 6\text{H}_2\text{O}$)
- Chromium nitrate ($\text{Cr}(\text{NO}_3)_3 \cdot 9\text{H}_2\text{O}$)
- Citric acid ($\text{C}_6\text{H}_8\text{O}_7 \cdot \text{H}_2\text{O}$)

- Ammonia
- Tetraethyl orthosilicate (TEOS)

We have used 99% pure chemicals for the preparation of $\text{CoCr}_2\text{O}_4/\text{SiO}_2$ nanoparticles. First, we found the desire ratio of cobalt nitrate, chromium nitrate and citric acid. Then we have obtained homogenous mixture by mixing chromium nitrate and cobalt nitrate of appropriate ratio in 30 ml solution of ethanol. This is solution A. After that we obtained second solution which is the mixture of distilled water, citric acid and TEOS with desired ratio (0 and 80%) of TEOS with total nitrate. This is solution B. Then we have inserted solution B in solution A drop wise with droplet and obtained a single solution C. Now we added ammonia in solution C drop wise to achieve its pH of 5. Then solution C is heated at 70°C under constant stirring until the formation of gel. After the formation of gel, it is placed in an oven at 110°C for 12 h. Afterwards, we have grind the material and then put it in the ceramic bottle and annealed at 900°C for 4 h and achieve desired $\text{CoCr}_2\text{O}_4/\text{SiO}_2$ nanoparticles. Flow chart of synthesis of $\text{CoCr}_2\text{O}_4/\text{SiO}_2$ is shown in Fig. 3.1.

TH: 18367

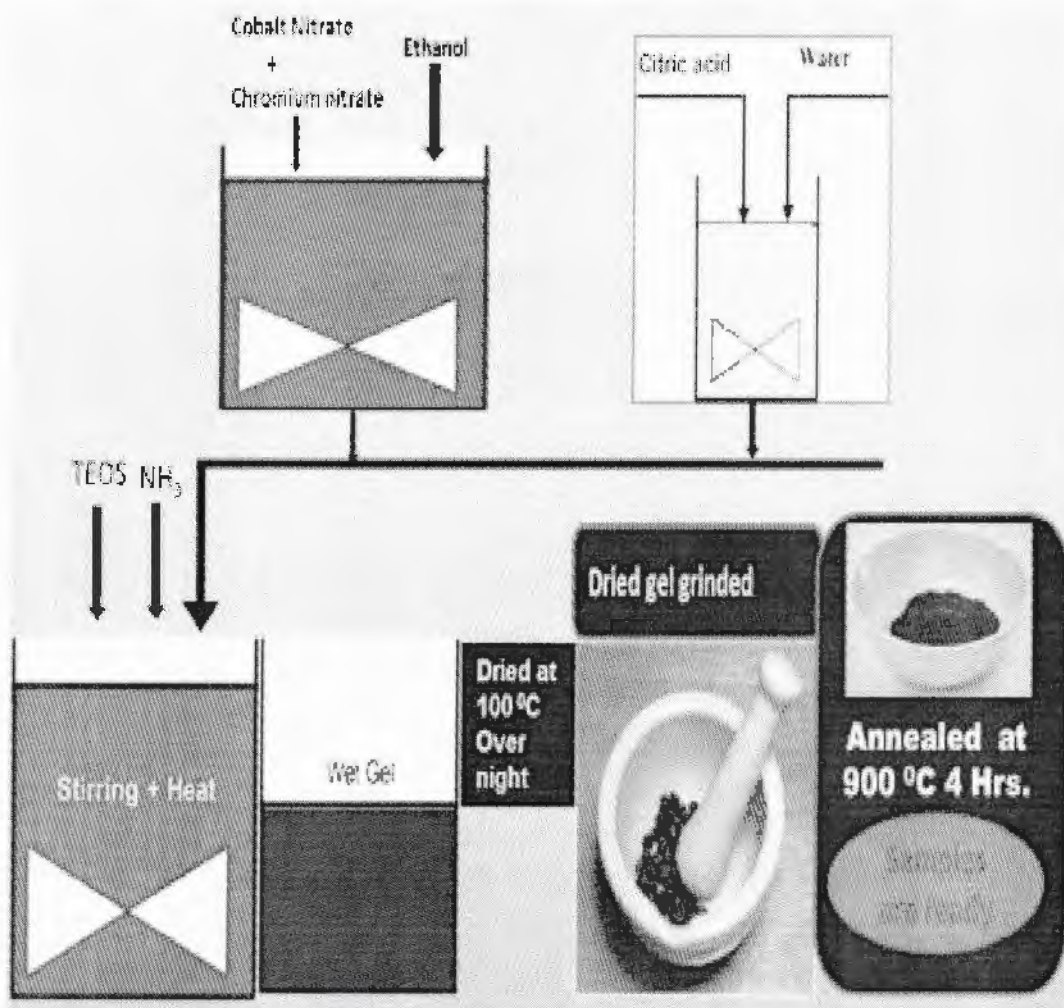


Fig:3.1(a) Synthesis of CoCr_2O_4 nanoparticles through sol-gel method.

3.3 Characterization Techniques

To study the different properties of SiO_2 coated CoCr_2O_4 nanoparticles we have to characterize our sample by using different techniques which are discussed below. SiO_2 coated CoCr_2O_4 nanoparticles were formed by sol-gel method. Determination of morphological, magnetic and structural properties involves different types of characterizing techniques such as,

- Transmission electron microscopy (TEM)
- X-ray diffraction (XRD)
- Superconducting quantum interference device (SQUID) magnetometer.

3.4 Transmission Electron Microscopy

Transmission electron microscopy (TEM) is a technique which is used to obtain information for shape and size of nanoparticles [97].

3.4.1 Working Principle of TEM

Typical parts of TEM are electron gun, stage, electromagnetic lens and florescent screen. TEM starts its working from electron gun and electron gun is considered as the main part of TEM. The highly energetic electrons are necessary for electron diffraction having energy 60-400 keV. Initially electrons are accelerated from cathode and move toward anode. A powerful lens is used behind the anode to condense the electrons into the shape of a beam and this beam is focused on the specimen. The specimen should be very thin like a thin film so that beam of electrons which is highly energetic can pass through the specimen.

When the beam of electrons pass through the specimen, it diffracts from its path and image of specimen is formed on the photographic film which is called screen. Schematic diagram of TEM is as shown in Fig. 3.2.

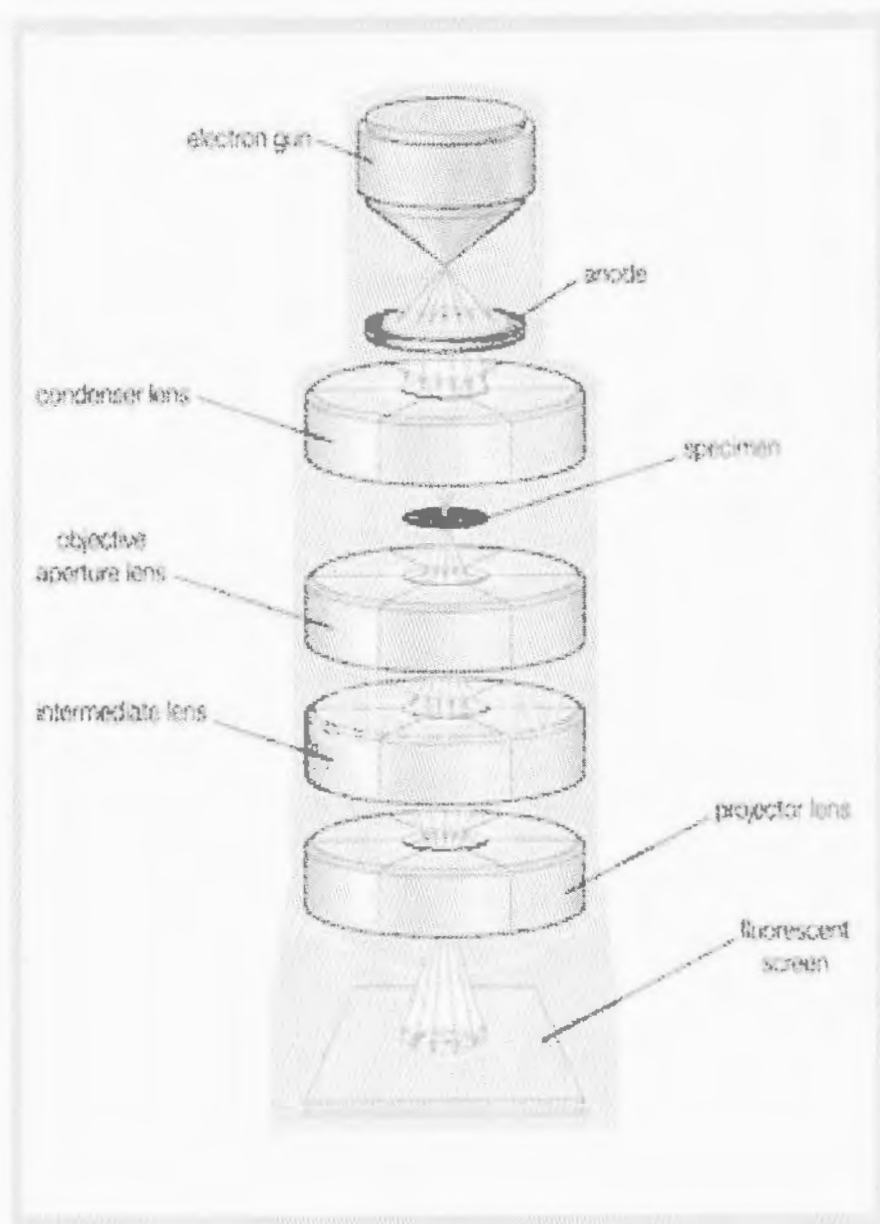


Fig. 3.2: TEM experimental setup [70]

3.5 X-Ray Diffraction (XRD)

XRD is a very significant technique and this technique is very helpful to find information about crystal structure of sample. By using this technique, we can study orientation, lattice constant, identification of material, geometry, defects and stresses etc. In this technique, the beam of x-ray directly falls on the sample and interacts with the sample. When the x-rays fall on the sample and scatter in different directions after the interaction. If constructive interference occurs between these scattered beams, then this constructive interference results a diffraction pattern as shown in Fig. 3.3.

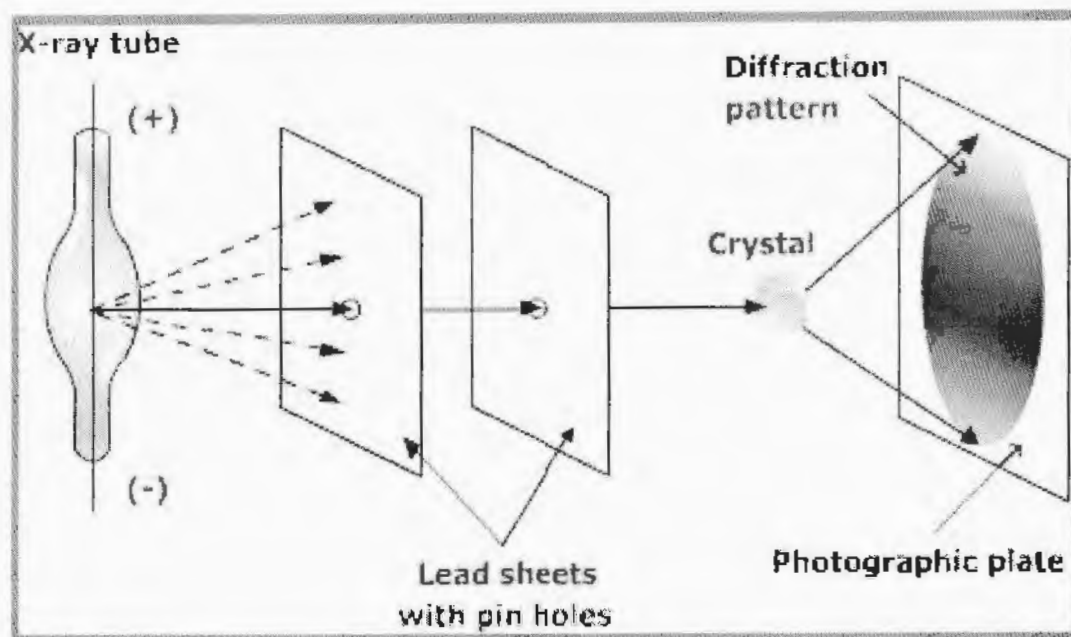


Fig. 3.3: X-Ray Diffraction [71]

3.5.1 Basic Principle of XRD

When x-ray beams collide with sample's atom, the electrons in the atoms vibrate with certain frequency due to force of beam. The frequency of electron is like the frequency of beams of x-ray which fall on the atom and interference occurs. There are two types of interference, one is constructive interference and other is destructive interference, in constructive interference electronic wave and x-ray beams are in phase and in destructive interference electronic wave and x-ray beams are out of phase. Constructive interference tells us that atoms are regularly arranged and structure of sample is periodic. Here we explain constructive interference by Bragg's law. Conditions for both constructive interference and destructive interference are shown in Fig. 3.4.

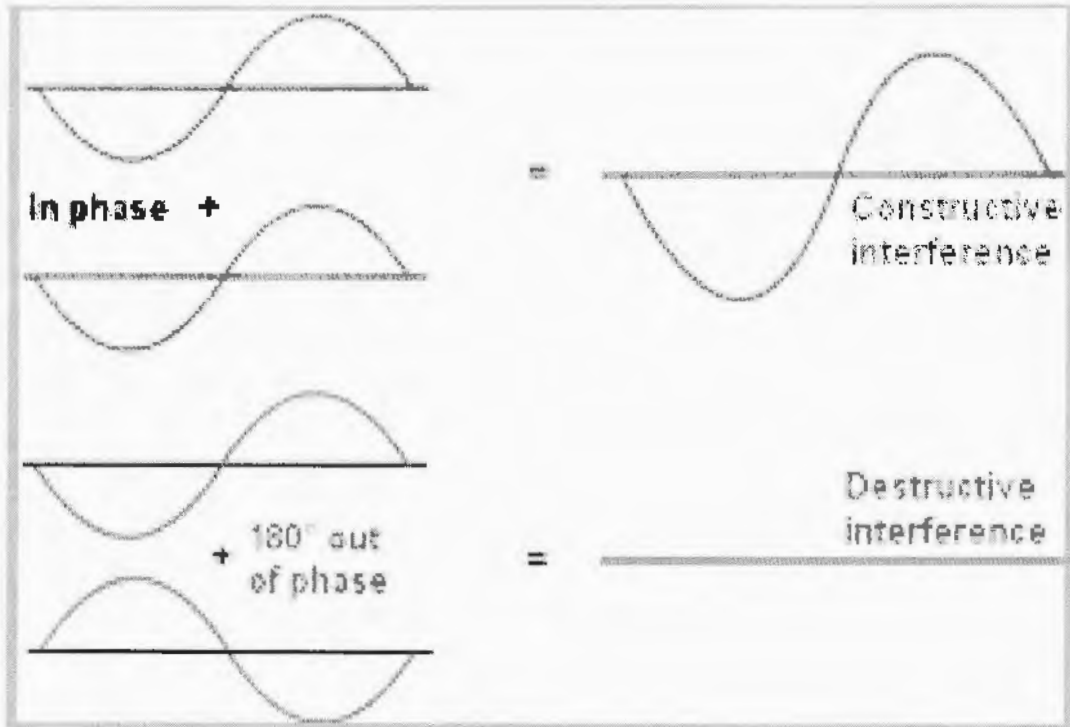


Fig. 3.4: Condition for constructive and destructive interference [72].

3.5.2 Bragg's Law

Bragg's law describes the condition on diffraction angle θ for the constructive interference to be at its maximum and mathematically it can be written as

$$n\lambda = 2d\sin\theta \quad (3.1)$$

In above equation λ is the wave length, θ is angle between scattered beam and surface of crystal, d is the distance between atomic plans in crystal and n is an integer ($n= 1, 2, 3 \dots$). Fig. 3.5 represents the Bragg's diffraction.

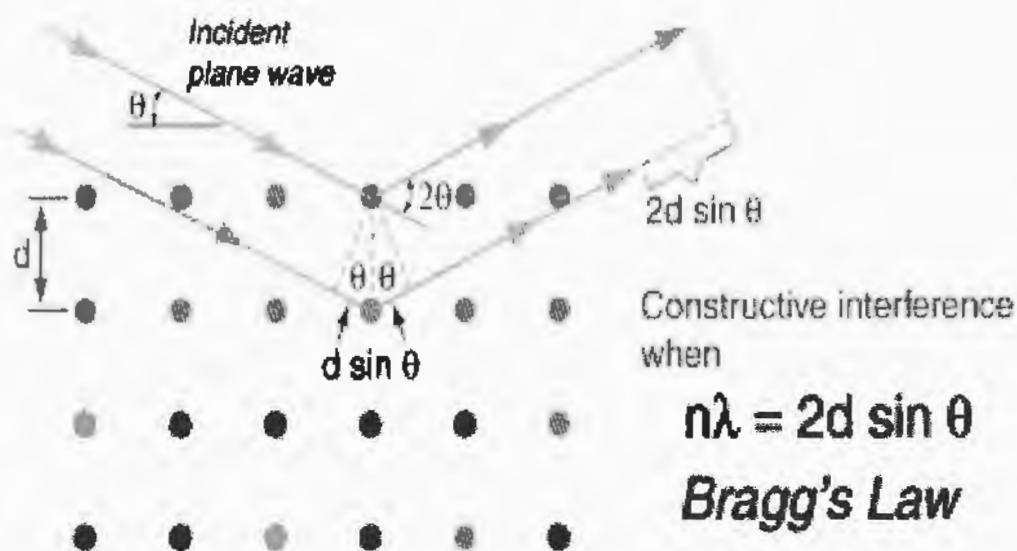


Fig. 3. 5: Representation of the Bragg's diffraction [73].

We can use x-ray beams for the information of crystal system i.e. to measure lattice parameter (a, b and c). Miller indices h, k, l for a plane of crystal system can be found by using this formula:

$$a = d / (h^2 + k^2 + l^2)^{1/2} \quad (3.2)$$

Scherrer's formula is used to find the crystallite size and it is given as

$$D = K\lambda / \beta \cos \theta_B \quad (3.3)$$

D = crystallite size

λ = X-ray wavelength

β = full width half maximum

θ_B = diffraction angle

K = Scherrer's constant

3.5.3 Applications of X-rays

XRD have lot of applications which are listed below:

Table 3.2: Uses and applications of XRD

Applications	Mainly use for
Identify	Crystalline orientation
	Grain size
Determine structure properties	Strain and epitaxy
	Crystalline plane
	Lattice parameter
	Phase composition

3.6 Superconducting Quantum Interference Device (SQUID) Magnetometer

Magnetic properties of nanoparticles are measured by using SQUID magnetometer. SQUID magnetometer contains two superconductors separated by a small distance and a thin insulating material fill the space between the superconductors. This device is capable for detecting very small magnetic field.

SQUID magnetometer possesses super conducting close loop and current flow in it. Super conducting close loop possess one or more Josephson junctions, shown in Fig. 3.6.

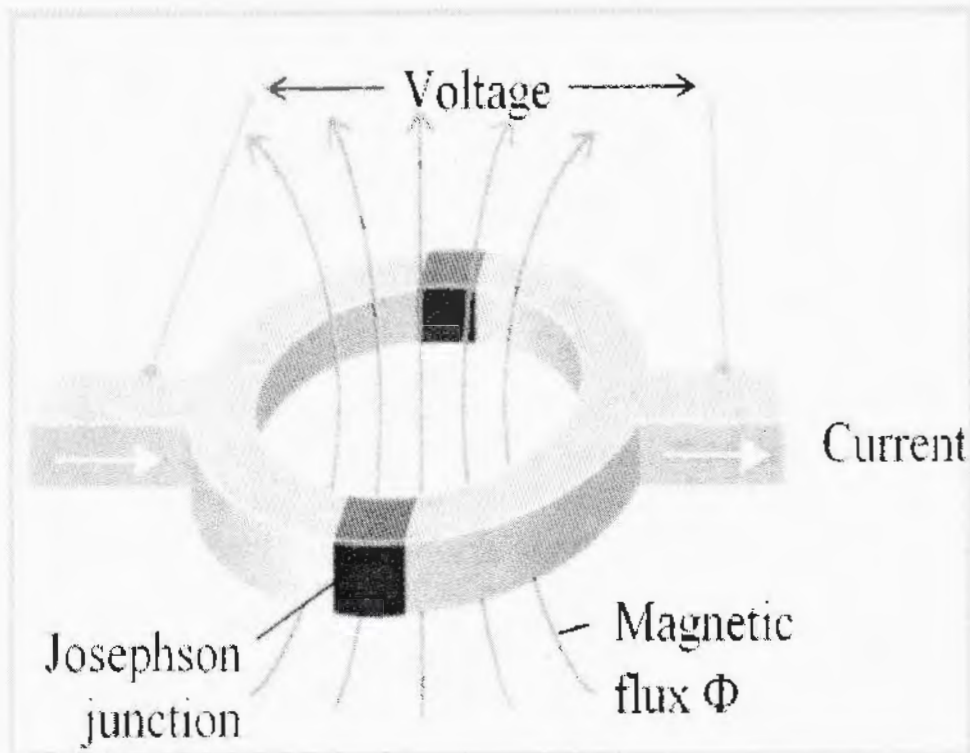


Fig. 3.6: Josephson junction [74].

This super conducting ring is in quantised state due to Josephson junction. Due to Josephson junction SQUID have ability to resolve the changes in the external magnetic field up to 10^{-15} T and it is shown in Fig. 3.7. SQUID magnetometers are also used to measure very large magnetic field and its maximum range is 7 T. For all above discussed reasons SQUID magnetometer is considered as very sensitive magnetometer. For the detection of magnetic field in the SQUID magnetometer sample moves in the superconducting coil and this coil detect the small change in the magnetic flux. Current in the detection coil is inductively coupled to SQUID sensors with the help of superconducting wires. Output voltage is directly proportional to current in the detection coil and SQUID works mainly current to voltage converter.

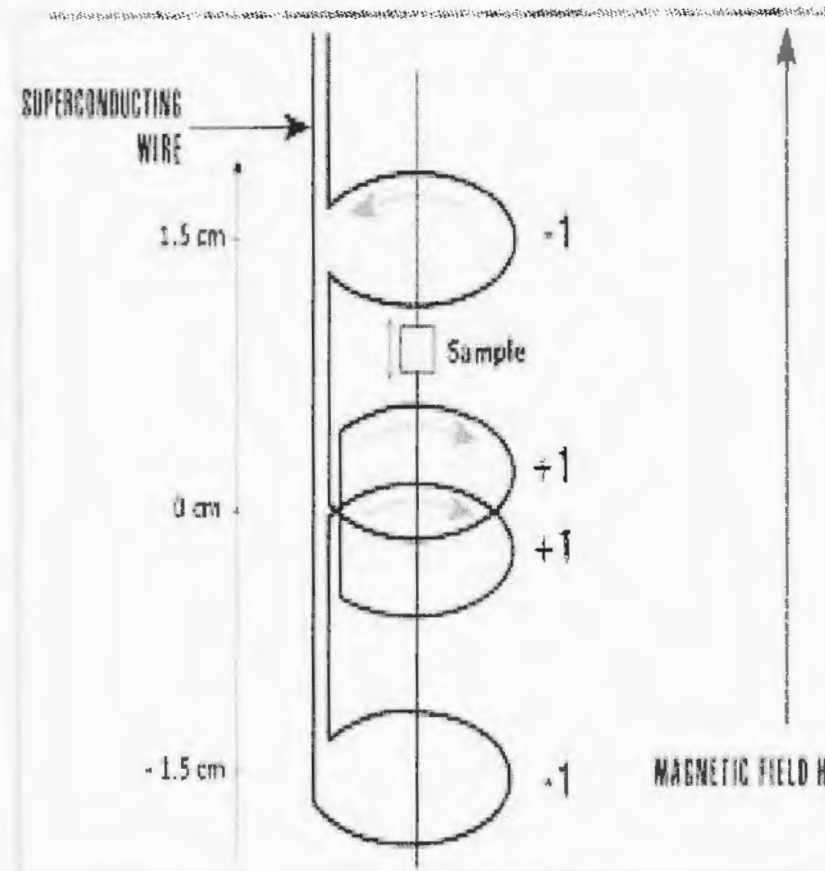


Fig. 3.7: Superconducting coil in SQUID [75].

CHAPTER 4

RESULTS AND DISCUSSION

Magnetically driven ferroelectric nanomaterials have been of great interest due to their physical properties and have potential applications in modern technology. In recent years, cobalt chromite (CoCr_2O_4) gains importance in scientific community due to its multiferroic (ferrimagnetic and ferroelectric) nature. CoCr_2O_4 nanoparticles exhibit spinel structure in which Co^{2+} ions reside on A sites and Cr^{3+} ions reside on B sites. The main problem in ferrimagnetic CoCr_2O_4 nanoparticles is the agglomeration due to strong interparticle interactions. To overcome this problem, we coated these magnetic nanoparticles with non-magnetic silica (SiO_2) material. We chose SiO_2 for surface coating which can control the particle size, interact with the surface spins, reduce the agglomeration, control the surface anisotropy and control the magnetic transitions [56].

In this research thesis, we have studied magnetic properties of uncoated and SiO_2 coated CoCr_2O_4 nanoparticles. Uncoated and SiO_2 coated CoCr_2O_4 nanoparticles have been synthesised by using sol gel method. X-ray diffraction characterization technique has used for the crystal structure of $\text{CoCr}_2\text{O}_4/\text{SiO}_2$ nanoparticles. Transmission electron microscope has used for the shape and size of nanoparticles. SQUID magnetometer has used for magnetic measurements.

4.1 X-Ray Diffraction

X-ray diffraction (XRD) is a very suitable and non-destructive technique to determine different parameters such as crystal structure, lattice parameter and crystallite size of nanoparticles. We have done XRD for $\text{CoCr}_2\text{O}_4/(\text{SiO}_2)_y$, $y = 0\%$ and $y = 80\%$ which are prepared by using sol-gel technique. Fig 4.1 shows the XRD scans of $\text{CoCr}_2\text{O}_4/\text{SiO}_2$ nanoparticles. Indexed peaks are (111), (220), (311), (400), (422), (511) and (440) revealed the normal spinel structure for both uncoated and coated CoCr_2O_4 nanoparticles. The positions of all peaks almost remain same for uncoated and SiO_2 coated nanoparticles, which proves that SiO_2 did not alter the internal

structure of CoCr_2O_4 nanoparticles. No peaks were found for SiO_2 because of its amorphous nature.

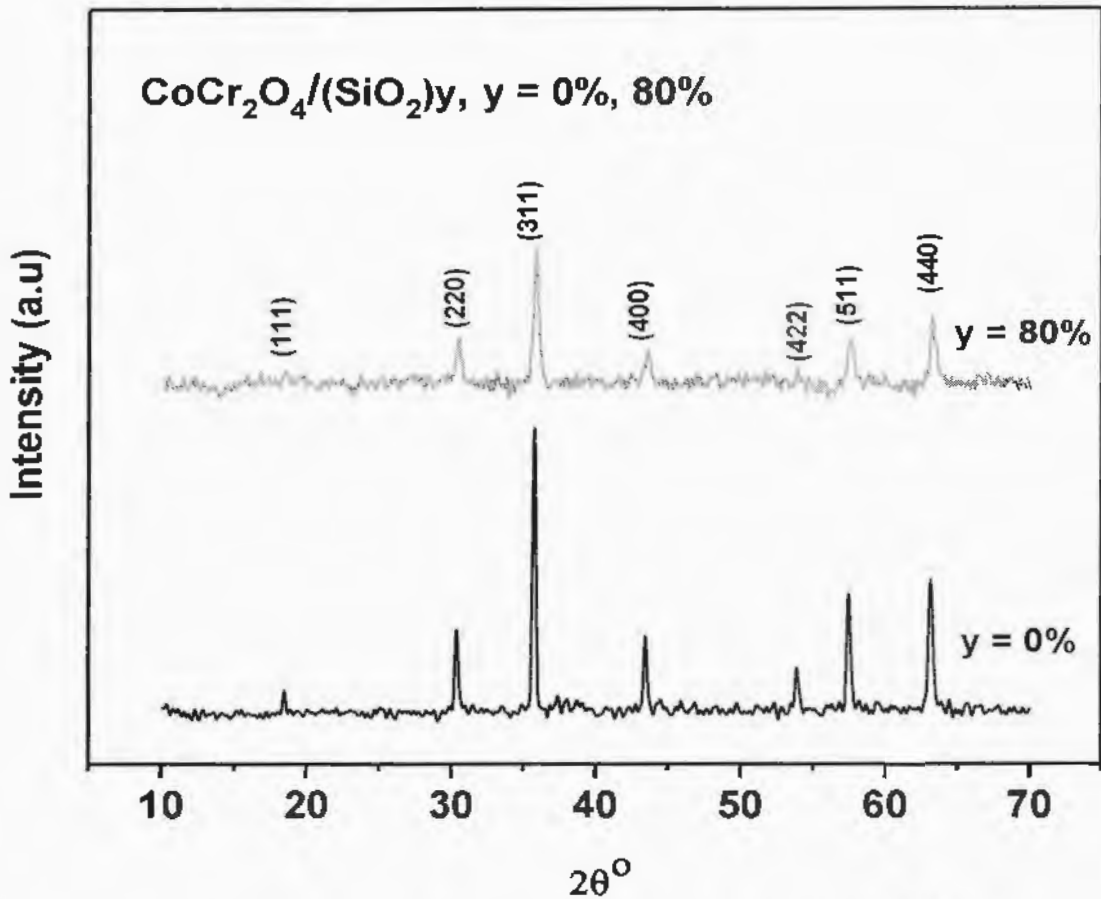


Fig. 4.1: XRD patterns of $\text{CoCr}_2\text{O}_4/(\text{SiO}_2)_y$ nanoparticles with $y = 0\%$ and 80% .

No impurity peaks have found in XRD which confirmed the single-phase of CoCr_2O_4 nanoparticles. The intensities of all the peaks have been reduced for coated nanoparticles. The average crystallite size of uncoated and 80% SiO_2 nanoparticles have been calculated by using Debye-Scherrer's formula (as given in eq. 4.1) by using main highest intensity peak (311).

$$D = \frac{0.9\lambda}{\beta \cos\theta} \quad (4.1)$$

Where D is the crystallite size, λ is the wavelength which is constant and its value is 0.1541 nm, β is the full width at half maximum (FWHM) and θ is the angle in degree. The average crystallite size of uncoated CoCr_2O_4 nanoparticle and 80% silica coated nanoparticle is 28 and 19 nm, respectively. The average crystallite size of uncoated nanoparticles is larger than coated nanoparticles. Size reduces for coated

nanoparticles because more nucleation sites were formed from SiO_2 matrix during the process of synthesis which stops the growth of nanoparticles [61, 76-78].

4.2 Transmission Electron Microscope

Transmission electron microscopy (TEM) is also used to look the size, shape and agglomeration in nanoparticles. Fig. 4.2 shows the TEM image of $\text{CoCr}_2\text{O}_4/\text{(SiO}_2\text{)}$ nanoparticles with 0% SiO_2 concentration. From Fig. 4.2, it is observed that the nanoparticles are of elongated/irregular shape. Some degree of agglomeration is also present due to magnetic interactions among nanoparticles [79, 80].

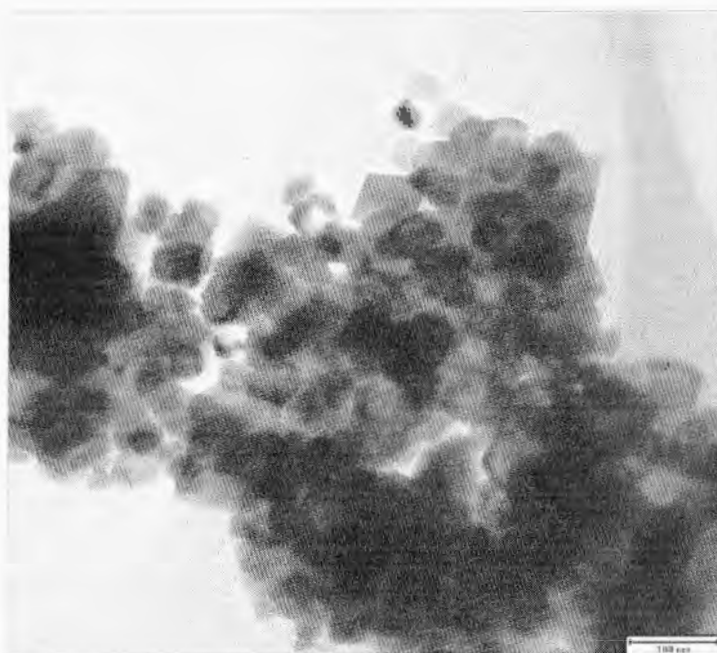


Fig. 4.2: TEM image of uncoated cobalt chromite nanoparticles at 100 nm scale.

4.3 Zero Field Cooled-Field Cooled Magnetization

Magnetic measurements of $\text{CoCr}_2\text{O}_4/\text{SiO}_2$ nanoparticles were taken by using superconductor quantum interference device (SQUID) magnetometer. Fig. 4.3 (a) and (b) shows the temperature dependent zero field cooled (ZFC) and field cooled (FC) magnetization curves for uncoated and 80% SiO_2 coated CoCr_2O_4 nanoparticles, respectively at different applied field such as 50, 500, and 1000 Oe. For ZFC curve, initially the sample was cooled from 145 K to 4.2 K with no external field and at 4.2

K magnetization is recorded with increasing temperature. As for as the FC curve is concerned, at 145 K temperature the sample was cooled by decreasing the temperature and magnetization is recorded in the presence of external magnetic field such as 50 Oe, 500 Oe and 1000 Oe [81]. The ZFC curves of uncoated and 80% SiO₂ coated CoCr₂O₄ nanoparticles show negative magnetization in the temperature range 4.2 K to 87 K and 4.2 K to 71 K, respectively due to uncompensated spins at the grain boundaries. The negative magnetization decreases in both uncoated and 80% SiO₂ coated CoCr₂O₄ nanoparticles by increasing the external magnetic field. As with the increase in external magnetic field, more magnetic moments aligned in the direction of magnetic field. From the graph of uncoated and 80% SiO₂ coated nanoparticles, it is observed that the negative magnetization also decreased when we coat the CoCr₂O₄ nanoparticles by SiO₂. It means that surface spins disorder of nanoparticles relaxed due to coating of SiO₂ [82-84]. The Curie temperature (T_C) in ZFC/FC is at which material changes from paramagnetic to ferrimagnetic material while the dip associated with T_S is a conical spiral state. ZFC/FC curves for uncoated CoCr₂O₄ nanoparticles revealed T_C at 99 K, 100 K and 101 K along with conical spiral state $T_S = 27$ K at 50 Oe, 500 Oe and 1000 Oe respectively. Plocek *et al.* and Plumier *et al.* [85, 86] obtained $T_C = 99$ K and $T_S = 26$ K for CoCr₂O₄ nanoparticles which confirms our ZFC/FC results. When we have coated the CoCr₂O₄ nanoparticles with silica, the values of T_C are 95 K, 99 K and 100 K along with conical spiral state T_S at 19 K, 25 K and 25 K at 50, 500 and 1000 Oe, respectively.

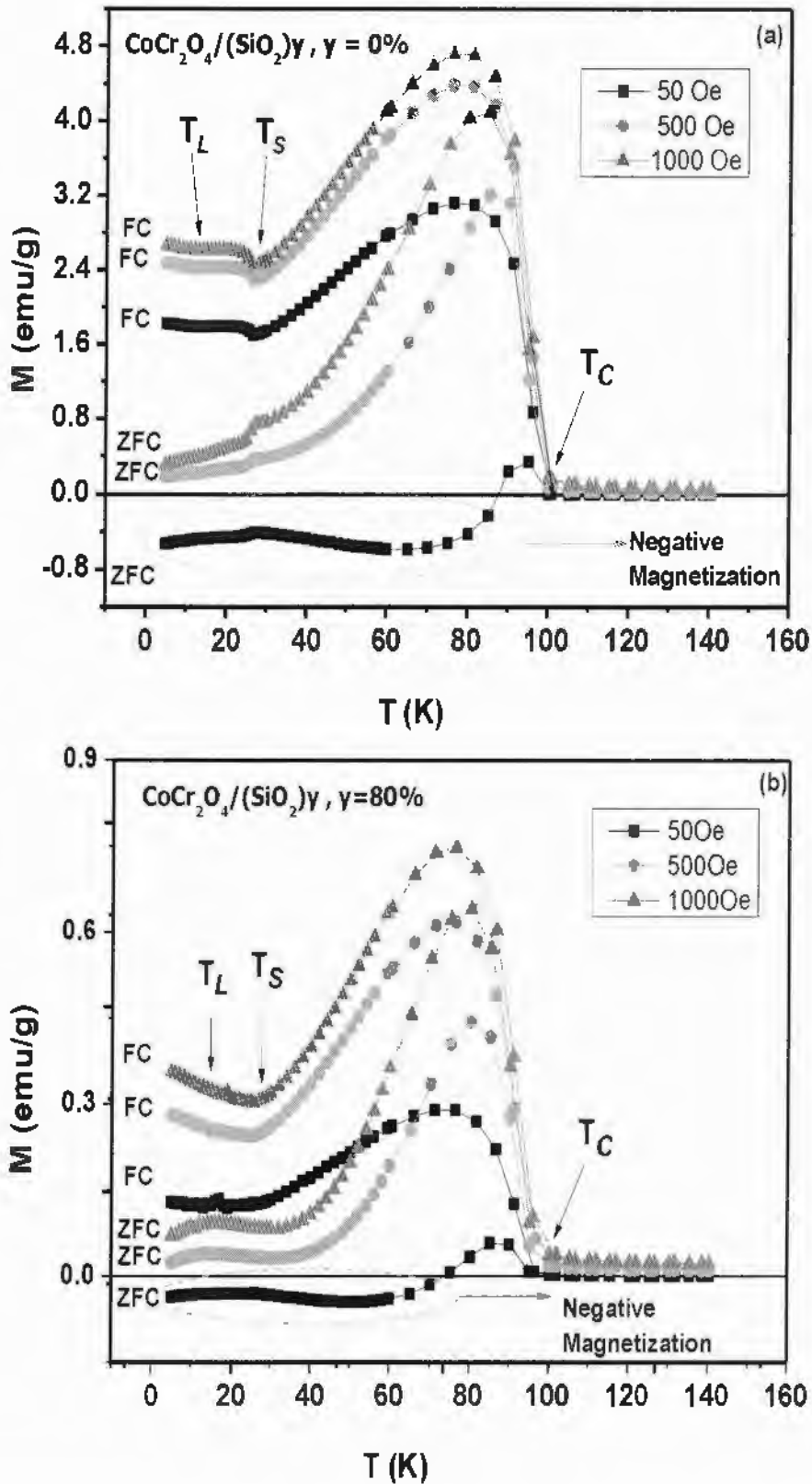


Fig. 4.3: ZFC and FC curves for (a) uncoated cobalt chromite nanoparticles and (b) silica coated cobalt chromite nanoparticles at different applied fields

Another low temperature state known as lock-in state occurs (at which spiral spins lock to lattice parameter) at $T_L = 12$ K for uncoated nanoparticles. For 80% SiO_2 coated nanoparticles, T_L occurs at 11.5 K, 15 K and 17 K under applied field 50 Oe, 500 Oe and 1000 Oe respectively. The values of T_S and T_L for uncoated CoCr_2O_4 nanoparticles are independent of field due to strong spin-lattice coupling at low temperatures [87]. The values of T_C , T_S and T_L are decreased for coated CoCr_2O_4 nanoparticles due to their decreased crystallite size as compared to uncoated nanoparticles [88, 89]. The values of T_C , T_S and T_L for uncoated and 80% SiO_2 coated CoCr_2O_4 nanoparticles at different field such as 50 Oe, 500 Oe and 1000 Oe are shown in table 4.1.

Table 4.1: The values of T_C , T_S and T_L for uncoated and 80% SiO_2 coated CoCr_2O_4 nanoparticles under different fields.

Concentration	Field	T_C	T_S	T_L
0%	50 Oe	99 K	27 K	12 K
	500 Oe	100 K	27 K	12 K
	1000 Oe	101 K	27 K	12 K
80%	50 Oe	95 K	19 K	11.5 K
	500 Oe	99 K	25 K	15 K
	1000 Oe	100 K	25 K	17 K

4.4 T-dependent M-H Loops of Uncoated Nanoparticles

We have taken temperature dependent M-H loops to study saturation magnetization (M_s) and coercivity (H_c) of CoCr_2O_4 nanoparticles due to surface and magnetic transitions effects. Fig. 4.4 depicts M-H loops of uncoated CoCr_2O_4 nanoparticles ($y = 0\%$) under ± 5 T field and at different temperatures at $T = 5$ K, 25 K, 50 K and 75 K. The inset of Fig. 4.4 reveals the expanded region for coercivity. All loops show ferrimagnetic trend which consist our ZFC/FC results. The M-H loops are not fully saturated at ± 5 T due to random surface spins of nanoparticles which need rather high field to get saturated.

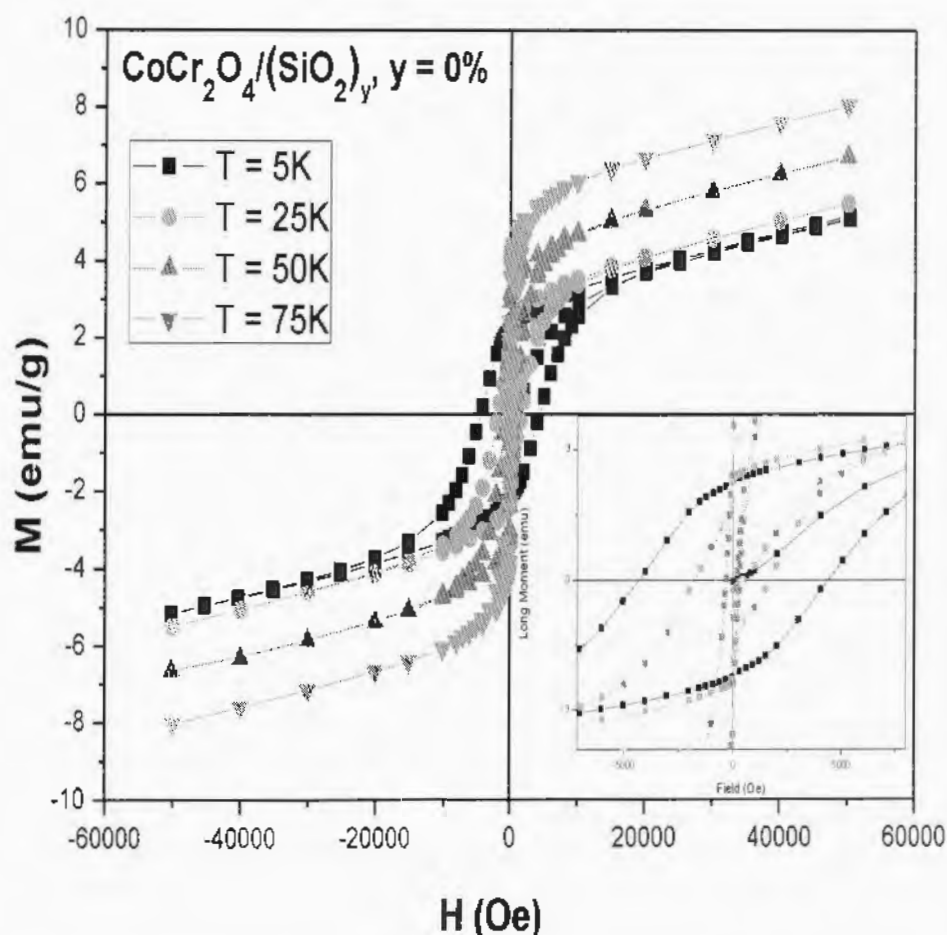


Fig. 4.4: M-H loops of uncoated CoCr_2O_4 nanoparticles at $T = 5\text{K}$, 25K , 50K and 75K .

From above Fig. 4.4, we find the value of parameters such as saturation magnetization (M_s) and coercivity (H_c). The value of saturation magnetization at 5 K temperature is $M_s = 5.1 \text{ emu/g}$. Fig 4.5 (a) shows M_s at different temperatures for uncoated CoCr_2O_4 nanoparticles. The value of M_s decreases with the decrease of temperature which is not according to Bloch's law prediction for ferro-ferrimagnetic materials. This trend attributes to presence of stiffed/strong conical spin spiral and lock-in states at low temperatures. We also note the value of coercivity (H_c) from M-H loops. Fig 4.5 (b) shows value of H_c at different temperatures. H_c shows increasing trend with decreasing the temperature due to decrease in thermal fluctuations [90-92]. At high temperatures, thermal energy is greater than anisotropic energy so spin flip time is less than measurement time so particle demonstrates lower value of coercivity. The thermal energy will decrease with decreasing the temperature and at low temperature thermal energy is less than anisotropic energy and exhibits higher value of coercivity.

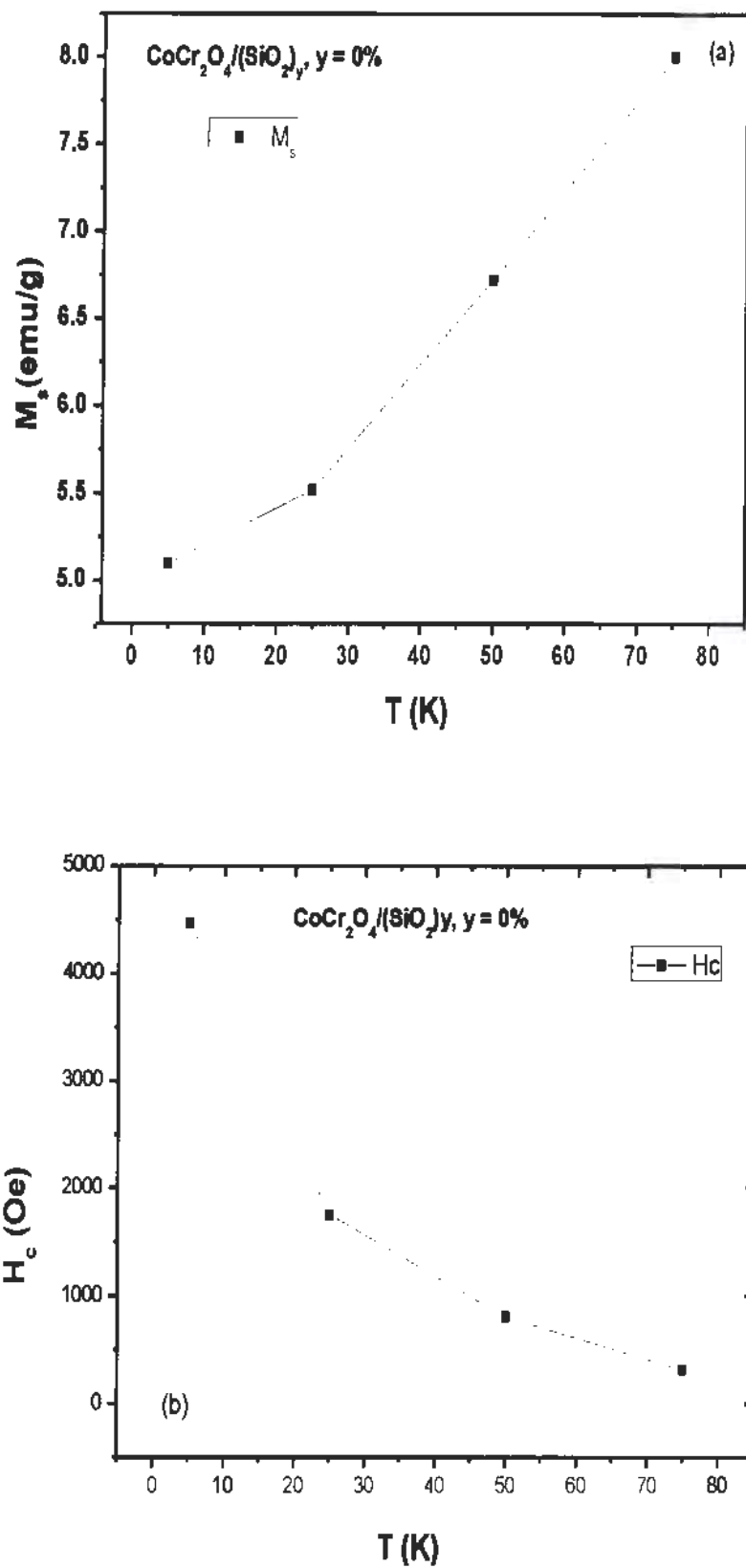


Fig. 4.5: (a) Variation in M_s and (b) H_c value with temperature of uncoated CoCr_2O_4 nanoparticles (solid lines just shows the trend)

4.4.1 T-dependent M-H Loops of SiO₂ Coated Nanoparticles

Fig. 4.6 shows that M-H loops of SiO₂ coated CoCr₂O₄ nanoparticles at different temperatures at T = 5 K, 15 K, 25 K, 50 K and 75 K. The value of saturation magnetization (M_s) at 5 K temperature is 2.16 emu/g. The value of M_s of uncoated nanoparticles is greater as compare to SiO₂ coated nanoparticles because crystallite size of uncoated nanoparticle is greater than SiO₂ coated nanoparticles. The value of M_s highly depends upon crystallite size. Smaller is the crystallite size, smaller will be the value of M_s . The reduction of M_s is also due to increasing the surface to volume ratio [93]. The M-H loops of SiO₂ coated CoCr₂O₄ nanoparticles at different temperature are less saturated even at high field 5 T as compare to uncoated nanoparticles due to surface effects.

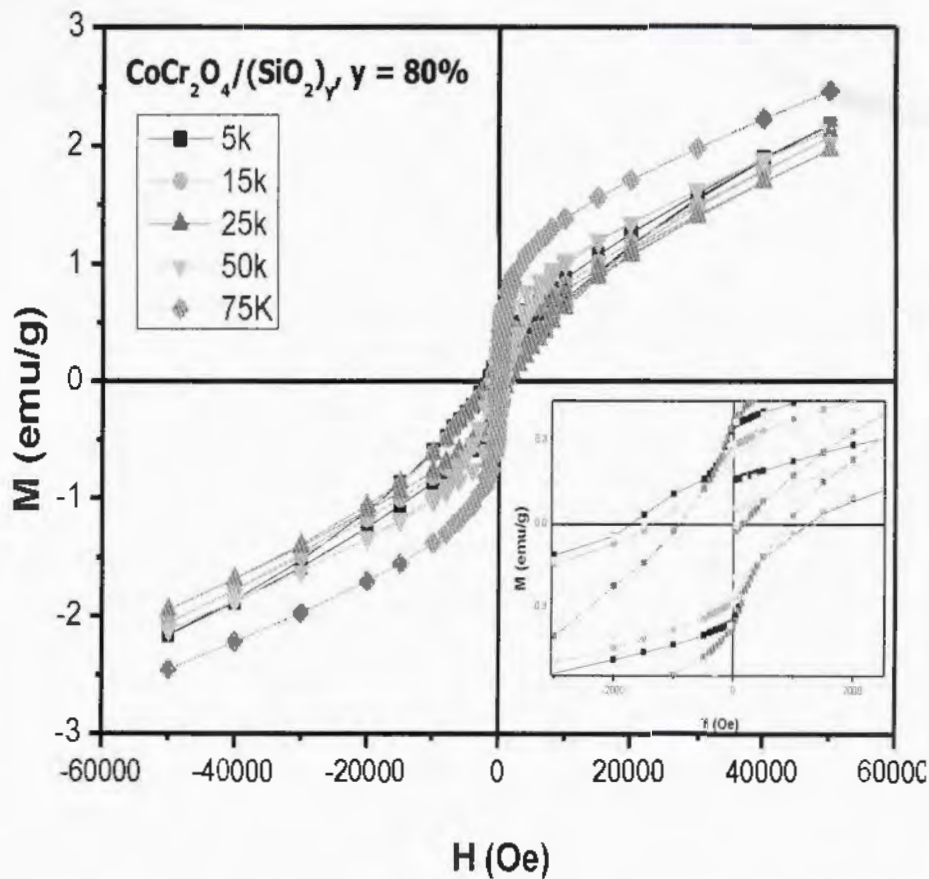
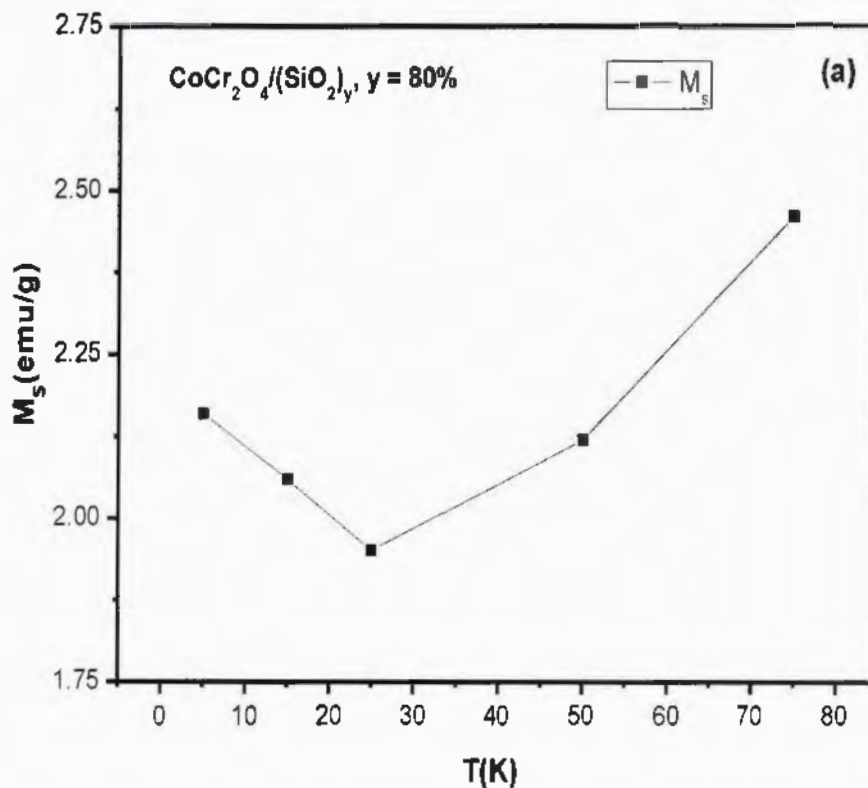


Fig. 4.6: M-H loops of SiO₂ coated CoCr₂O₄ nanoparticles (with $y = 80\%$) at T = 5K, 15K, 25K, 50K and 75K.

Fig 4.7(a) shows M_s value of SiO₂ coated nanoparticles at different temperatures. From M-H loops of SiO₂ coated CoCr₂O₄ nanoparticles, the value of M_s

of SiO₂ coated nanoparticles shows abnormal behaviour with temperature due to non-magnetic SiO₂ coating. The SiO₂ coating can enhance surface disorder by creating a surrounding layer around the nanoparticles [94]. There is an increase in M_s value below 25 K which is attributed to change in spin-spiral state due to SiO₂ coating. Fig. 4.7 (b) shows the T-dependent H_c for uncoated and SiO₂ coated cobalt chromite nanoparticles. The value of H_c also shows increasing with decreasing temperature for SiO₂ coated nanoparticles. H_c of nanoparticles depends upon the many factors such as size of particle, core anisotropy, dipole interaction, coating material, surface anisotropy and annealing temperature [95].



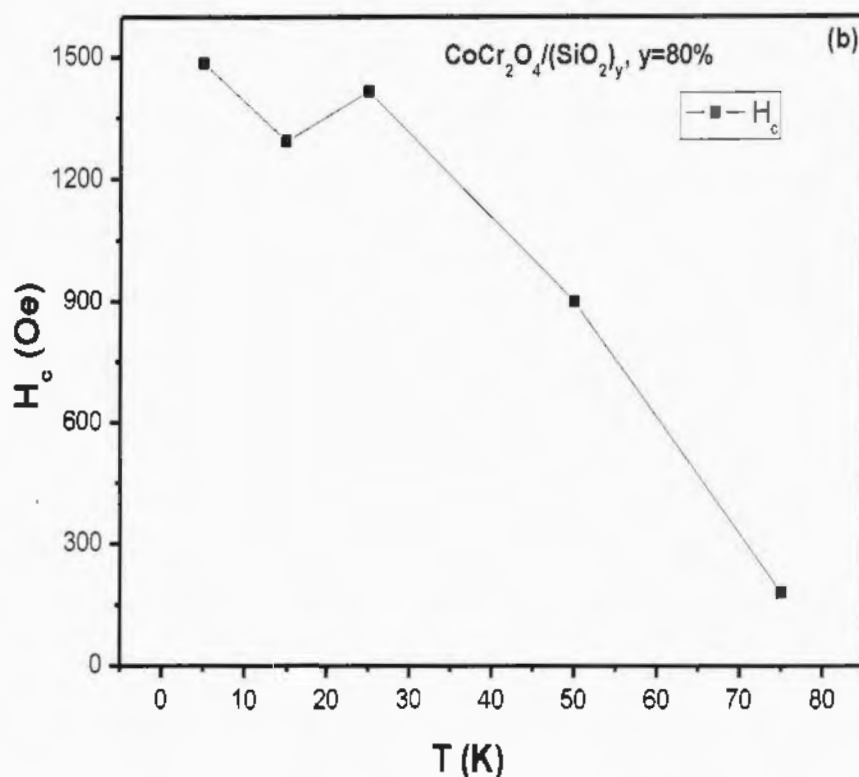


Fig. 4.7: (a) Variation in M_s and (b) H_c value with temperature of silica coated nanoparticles (solid lines just show the trend).

4.4.2 H_c and M_s for Uncoated and Silica Coated Nanoparticles

Fig 4.8 (a) shows the combine graph of M_s with temperature for both uncoated and SiO_2 coated CoCr_2O_4 nanoparticles. The behaviour of M_s with temperature for SiO_2 coated nanoparticles is different from uncoated nanoparticles. Below $T = 25$ K, the value of M_s for uncoated nanoparticles is decreasing with decreasing temperature while it is increasing with decreasing temperature for SiO_2 coated nanoparticles. This region is conical spin spiral region where both electric dipoles and magnetic dipoles are present at the same phase.

Fig 4.8 (b) shows combine H_c with temperature for both uncoated and SiO_2 coated CoCr_2O_4 nanoparticles. From this, the behaviour of H_c with temperature for uncoated CoCr_2O_4 nanoparticles was changed with SiO_2 coating. The sharp increase in H_c in uncoated nanoparticles is not observed in SiO_2 coated nanoparticles which means that surface anisotropy is decreased in coated nanoparticles.

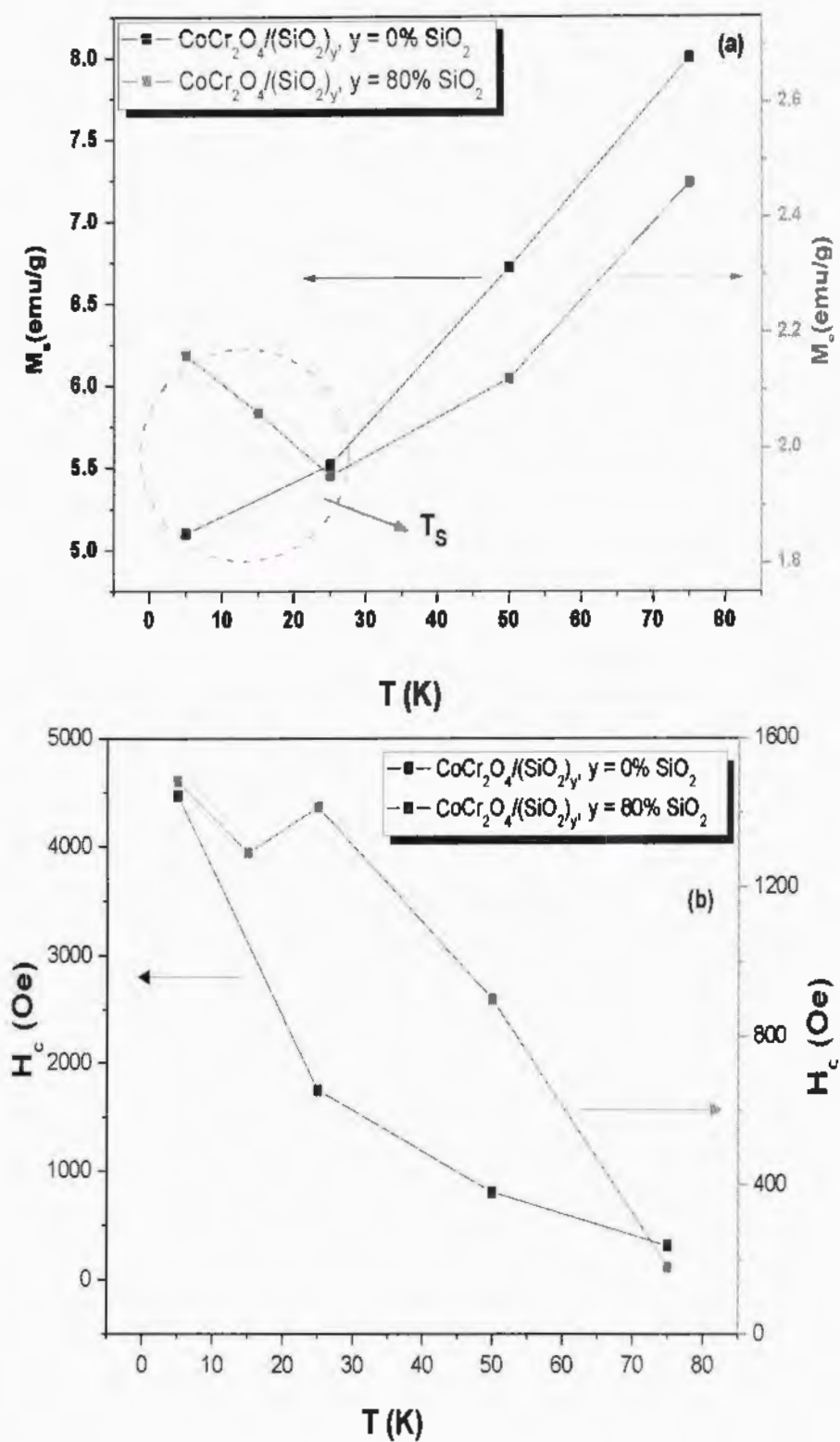


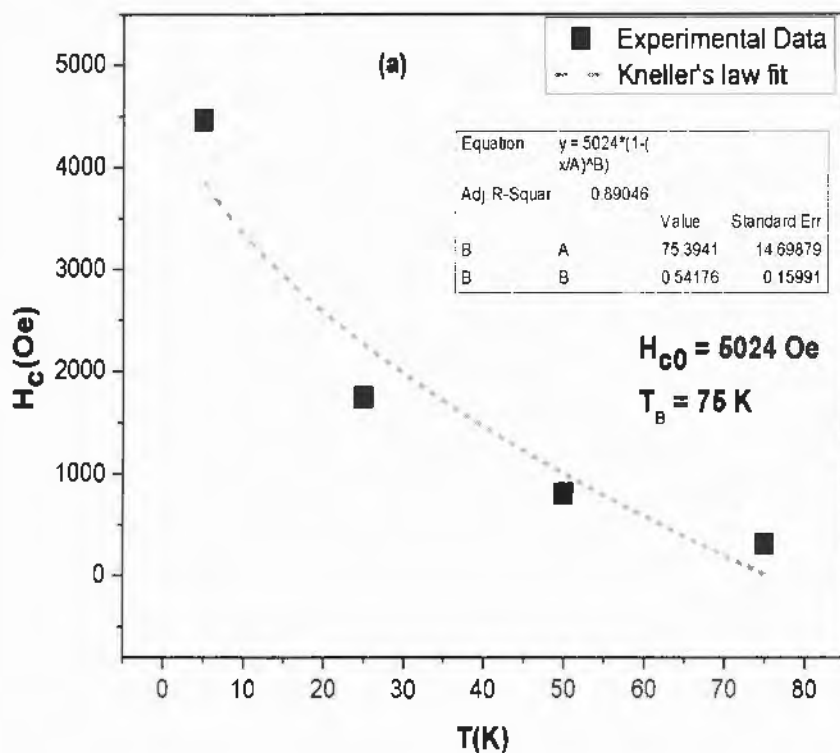
Fig. 4.8: (a) M_s vs. T and (b) H_c vs. T of uncoated and SiO_2 coated CoCr_2O_4 nanoparticles (solid lines just show the trend).

4.5 Kneller's Law fitting

The experimental H_c data of uncoated and SiO_2 coated CoCr_2O_4 nanoparticles is fitted by using Kneller's law. The coercivity for randomly oriented non-interacting nanoparticles (single domain and uniaxial anisotropy) can be explained by using Kneller's law [96] as given below,

$$H_c = H_{c0} [1-(T/T_B)^\alpha] \quad (4.2)$$

Where H_c is coercivity at any temperature, H_{c0} is the coercivity at temperature $T = 0$ K and T_B is average blocking temperature. Fig. 4.9 (a) and (b) shows the fitting of Kneller's law for uncoated and SiO_2 coated CoCr_2O_4 nanoparticles. Kneller's law best fit for uncoated nanoparticles reveals fitting parameters as $T_B = 75$ K, $\alpha = 1.54$ and for SiO_2 coated nanoparticles having $T_B = 81$ k and $\alpha = 1.59$. Kneller's law diverges at lower temperatures for uncoated nanoparticles due to strong interparticle interactions or/and surface disorder [97].



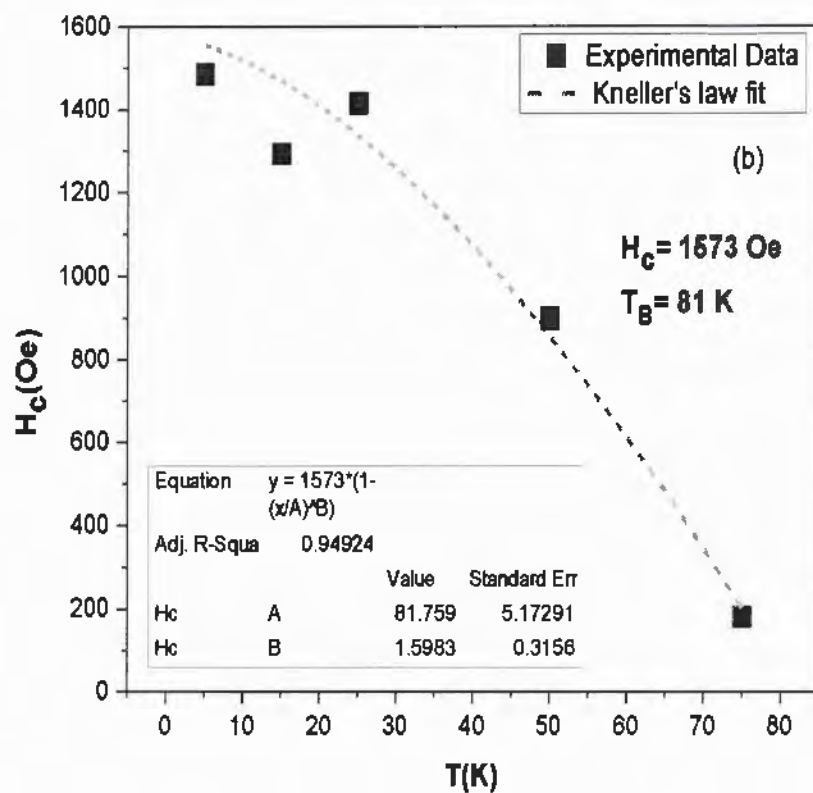


Fig. 4.9: (a) Kneller's law fit for uncoated and (b) SiO_2 coated CoCr_2O_4 nanoparticles.

Conclusions

Temperature dependent magnetic properties of uncoated and SiO₂ coated CoCr₂O₄ nanoparticles were studied in detail. XRD patterns reveal normal spinel structure for both uncoated and SiO₂ coated nanoparticles. The average crystallite size is decreased for SiO₂ coated nanoparticles due to presence of amorphous SiO₂ which restricts the growth of nanoparticles. ZFC/FC curves of uncoated and SiO₂ coated CoCr₂O₄ nanoparticles at 50, 500 and 1000 Oe have been studied. The values of T_c were 99, 100 and 101 K for uncoated nanoparticles at 50, 500 and 1000 Oe, respectively. For SiO₂ coated nanoparticles, T_c was 95, 99 and 100 K at 50 Oe, 500 Oe and 1000 Oe, respectively. The values of T_s = 27 K and T_L = 12 K for uncoated nanoparticles are found field independent due to strong lattice coupling as compared to SiO₂ coated nanoparticles. ZFC curve of uncoated CoCr₂O₄ nanoparticles shows negative magnetization which persists up to 87 K due to existence of uncompensated spin at grain boundaries and this negative magnetization is decreased for SiO₂ coated nanoparticles. The value of M_s is decreasing with decreasing temperature for uncoated nanoparticles and shows abnormal behaviour for coated nanoparticles due to amorphous SiO₂ coating. Below 25 K, the value of M_s for uncoated nanoparticles is decreasing while it is increasing for SiO₂ coated nanoparticles. H_c shows increasing trend with decreasing temperature for both concentration due to decrease in thermal fluctuations at low temperatures. The experimental H_c data of uncoated and SiO₂ coated nanoparticles has been fitted by using Kneller's law. The fitting parameters are T_B = 75 K, α = 0.54 for uncoated CoCr₂O₄ nanoparticles and T_B = 81 K, α = 1.59 are for SiO₂ coated CoCr₂O₄ nanoparticles. In conclusion, SiO₂ coating interferes with the disordered spin-spiral state ordering and decreasing surface effects in these chromite nanoparticles.

References

- [1] T. Rogers-Hayden, N. Pidgeon, Moving engagement “upstream”? Nanotechnologies and the Royal Society and Royal Academy of Engineering's inquiry, *Public Understanding of Science*, **16** (2007) 345-364.
- [2] http://www.academia.edu/28610401/nanopartikel_applied.
- [3] G.A. Mansoori, *Principles of nanotechnology: molecular-based study of condensed matter in small systems*, World Scientific Publishing Co Inc, 2005.
- [4] <https://www.hdiac.org/node/1907>.
- [5] <http://nano--tech.blogspot.com/p/history.html>.
- [6] R.R.M.e.N.M.i.C.e. Klabunde K.J., Wiley, 2009)(ISBN 0470222700)(O)(807s)_Ch_.pdf.
- [7] <https://www.slideshare.net/AhmedTaha67/nanotechnology-46040729>.
- [8] E. Bingham, G. Lindén, Helsinki Institute for Information Technology HIIT.
- [9] C.Q. Sun, B. Tay, S. Li, X. Sun, S. Lau, T. Chen, Bandgap expansion of a nanometric semiconductor, *Materials Phy and Mech*, **4** (2001) 129-133.
- [10] A. Gusev, *Nanomaterials, nanostructures, nanotechnologies*, Fizmatlit, Moscow, (2007) 416.
- [11] <http://eng.thesaurus.rusnano.com/wiki/article1371>.
- [12] I.i. nanomaterials-sisu.pdf.
- [13] <http://vtu.ac.in/nano-technology/>.
- [14] P. Babalola, A. Inegbenebor, C. Bolu, A. Inegbenebor, The Development of Molecular-Based Materials for Electrical and Electronic Applications, *J. (TMS)*, **67** (2015) 830-833.
- [15] D.J. Griffiths, Resource letter EM-1: Electromagnetic momentum, *Am. J. Phys.* **80** (2012) 7-18.
- [16] T. Pang, An introduction to computational physics, in, AAPT, 1999.
- [17] M. Bruce, Domain Theory, Hitchhiker's Guide to Magnetism for the Environmental Magnetism Workshop, Institute for Rock Magnetism. http://www.irm.umn.edu/hg2m/hg2m_d/hg2m_d.html, (1991).

- [18] <http://www.xamidea.in/learning/chemistry/22/amines/9/magnetic-properties-of-solids/title/10000126>.
- [19] P. Tsai, Synthesis and Characterization of Ferromagnetic Nanowires, (2011).
- [20] <http://www.splung.com/content/sid/3/page/magnetism>.
- [21] https://www.researchgate.net/figure/263785799_fig10_Figure-35-Atomic-dipole-configurations-for-a-diamagnetic-material.
- [22] <http://nptel.ac.in/courses/115103039/module1/lec1/3.html>.
- [23] S. Blundell, Magnetism in Condensed Matter (Oxford master series in condensed matter physics), Oxford University Press, 2001.
- [24] <https://www.linkedin.com/pulse/measuring-principle-oxygen-through-paramagnetic-property-fontes>.
- [25] <http://eu.wiley.com/WileyCDA/WileyTitle/productCd-EHEP000803.html>.
- [26] http://www.irm.umn.edu/hg2m/hg2m_b/hg2m_b.html.
- [27] <http://www.allegromicro.com/en/Design-Center/Technical-Documents/Hall-Effect-Sensor-IC-Publications/Hysteresis-Mitigation-in-Current-Sensor-ICs-Using-Ferromagnetic-Cores.aspx>.
- [28] <https://en.wikipedia.org/wiki/Antiferromagnetism>.
- [29] <http://sciexplorer.blogspot.com/2011/10/magnetism-explained-4-other-kinds-of.html>.
- [30] T. Sato, T. Iijima, M. Seki, N. Inagaki, Magnetic properties of ultrafine ferrite particles, *J. Magn Magn Mater.* **65** (1987) 252-256.
- [31] <https://www.ncbi.nlm.nih.gov/pmc/articles/PMC2811286/>.
- [32] H. Schmidt, Nanoparticles by chemical synthesis, processing to materials and innovative applications, *Applied organometallic chemistry*, **15** (2001) 331-343.
- [33] S. Dey, A. Roy, J. Ghose, R. Bhowmik, R. Ranganathan, Size dependent magnetic phase of nanocrystalline $\text{Co}_{0.2}\text{Zn}_{0.8}\text{Fe}_2\text{O}_4$, *J. Appl. Phys.* **90** (2001) 4138-4142.
- [34] V.I. Kalikmanov, Statistical thermodynamics of ferrofluids, *Physica A: Statistical Mechanics and its Applications*, **183** (1992) 25-50.
- [35] M. Veverka, P. Veverka, O. Kaman, A. Lančok, K. Závěta, E. Pollert, K. Knížek, J. Boháček, M. Beneš, P. Kašpar, Magnetic heating by cobalt ferrite nanoparticles, *Nanotechnology*, **18** (2007) 345704.
- [36] <https://en.wikipedia.org/wiki/Superparamagnetism>.

- [37] L. Néel, S. Robin, B. Vodar, J.-P. Mathieu, L. Couture-Mathieu, L. Lafourcade, R. Dargent, J. Wucher, J.M.T. Vidal, A. Rousset, Theory of magnetic viscosity by diffusion Théorie du trainage magnétique de diffusion p. 249, *J Phys. et le Radium*, **13** (1952).
- [38] E. Tronc, J. Jolivet, J. Dormann, D. Fiorani, Magnetic Properties of Fine Particles, in, North-Holland, Amsterdam, 1992.
- [39] D. Dickson, N. Reid, C. Hunt, H. Williams, M. El-Hilo, K. O'Grady, Determination of f_0 for fine magnetic particles, *J. Magn. Magn. Mater*, **125** (1993) 345-350.
- [40] M. Ziese, Extrinsic magnetotransport phenomena in ferromagnetic oxides, *Reports on Progress in Physics*, **65** (2002) 143
- [41] H.G. Vogel, Antidiabetic activity, in: *Drug Discovery and Evaluation*, Springer, 2008, pp. 1323-1607.
- [42] A J. Rondinone, A C. Samia, Z.J. Zhang, Characterizing the magnetic anisotropy constant of spinel cobalt ferrite nanoparticles, *Applied Physics Letters*, **76** (2000) 3624-3626
- [43] N.M. Abdul-Ameer, M.C. Abdulrida, Direct optical energy gap in amorphous silicon quantum dots, *Journal of Modern Physics*, **2** (2011) 1530.
- [44] S. Azzuhri, W. Mahadi, Power transmission line magnetic fields: a survey on 120 kV overhead power transmission lines in Malaysia, in: *TENCON 2004. 2004 IEEE Region 10 Conference*, IEEE, 2004, pp. 421-424.
- [45] <https://en.wikipedia.org/wiki/Magnetochemistry>.
- [46] <http://www.electronics-tutorials.ws/electromagnetism/magnetic-hysteresis.html>.
- [47] D S. Mathew, R.-S. Juang, An overview of the structure and magnetism of spinel ferrite nanoparticles and their synthesis in microemulsions, *Chemical Engineering Journal*, **129** (2007) 51-65.
- [48] A B. Van Groenou, P. Bongers, A. Stuyts, Magnetism, microstructure and crystal chemistry of spinel ferrites, *Materials Science and Engineering*, **3** (1969) 317-392.
- [49] <http://www.cdti.com/spinel/>.
- [50] Y. Han, W. Liu, P. Wu, X. Xu, M. Guo, G. Rao, S. Wang, Effect of aliovalent Pd substitution on multiferroic properties in BiFeO₃ nanoparticles, *J. Alloys Compd.* **661** (2016) 115-121.

- [51] X. Ming, Q. Hu, F. Hu, F. Du, Y. Wei, G. Chen, Potential multiferroic materials of Fe-substituted BiCoO₃: An ab initio study, *Computational Materials Science*, **119** (2016) 33-40.
- [52] M.K. Sharif, M.A. Khan, A. Hussain, F. Iqbal, I. Shakir, G. Murtaza, M.N. Akhtar, M. Ahmad, M.F. Warsi, Synthesis and characterization of Zr and Mg doped BiFeO₃ nanocrystalline multiferroics via micro emulsion route, *J. Alloys Compd.* **667** (2016) 329-340.
- [53] D.-J. Huang, J. Okamoto, S.-W. Huang, C.-Y. Mou, Magnetic transitions of multiferroic frustrated magnets revealed by resonant soft x-ray magnetic scattering, *Journal of the Physical Society of Japan*, **79** (2010) 011009.
- [54] A. Knyazev, M. Maćzka, E. Bulanov, M. Ptak, S. Belopolskaya, High-temperature thermal and X-ray diffraction studies, and room-temperature spectroscopic investigation of some inorganic pigments, *Dyes and Pigments*, **91** (2011) 286-293.
- [55] E.H. Kim, H.S. Lee, B.K. Kwak, B.-K. Kim, Synthesis of ferrofluid with magnetic nanoparticles by sonochemical method for MRI contrast agent, *J. Magn. Mater.* **289** (2005) 328-330.
- [56] K. Nadeem, L. Ali, I. Gul, S. Rizwan, M. Mumtaz, Effect of silica coating on the structural, dielectric, and magnetic properties of maghemite nanoparticles, *J. Non-Cryst Solids*, **404** (2014) 72-77.
- [57] K. Nadeem, F. Zeb, M.A. Abid, M. Mumtaz, M.A. ur Rehman, Effect of amorphous silica matrix on structural, magnetic, and dielectric properties of cobalt ferrite/silica nanocomposites, *J. Non-Cryst. Solids*. **400** (2014) 45-50.
- [58] K. Nadeem, T. Traussnig, I. Letofsky-Papst, H. Krenn, U. Brossmann, R. Wüschum, Sol-gel synthesis and characterization of single-phase Ni ferrite nanoparticles dispersed in SiO₂ matrix, *J. Alloys Compd.* **493** (2010) 385-390.
- [59] J. Nogués, J. Sort, V. Langlais, V. Skumryev, S. Surinach, J. Muñoz, M. Baró, Exchange bias in nanostructures, *Physics Reports*, **422** (2005) 65-117.
- [60] T. Moran, J. Nogués, D. Lederman, I.K. Schuller, Perpendicular coupling at Fe-FeF₂ interfaces, *Applied Physics Letters*, **72** (1998) 617-619.
- [61] M. Kamran, A. Ullah, Y. Mehmood, K. Nadeem, H. Krenn, Role of SiO₂ coating in multiferroic CoCr₂O₄ nanoparticles, *AIP Advances*, **7** (2017) 025011.

- [62] M. Kamran, A. Ullah, S. Rahman, A. Tahir, K. Nadeem, M.A. ur Rehman, S. Hussain, Structural, magnetic, and dielectric properties of multiferroic $\text{Co}_{1-x}\text{Mg}_x\text{Cr}_2\text{O}_4$ nanoparticles, *J. Magn. Magn. Mater.*, **433** (2017) 178-186.
- [63] R. Stamps, Mechanisms for exchange bias, *J. Phys. D: Appl. Phys.*, **33** (2000) R247
- [64] S. Joshi, M. Kumar, S. Chhoker, G. Srivastava, M. Jewariya, V. Singh, Structural, magnetic, dielectric and optical properties of nickel ferrite nanoparticles synthesized by co-precipitation method, *J. Molecular Structure*, **1076** (2014) 55-62.
- [65] M. Atif, M. Nadeem, R. Grössinger, R.S. Turtelli, Studies on the magnetic, magnetostrictive and electrical properties of sol-gel synthesized Zn doped nickel ferrite, *J. Alloys Compd.*, **509** (2011) 5720-5724.
- [66] B. Martinez, X. Obradors, L. Balcells, A. Rouanet, C. Monty, Low temperature surface spin-glass transition in $\gamma\text{-Fe}_2\text{O}_3$ nanoparticles, *Physical review letters*, **80** (1998) 181.
- [67] E. Eftaxias, K. Trohidou, Numerical study of the exchange bias effects in magnetic nanoparticles with core/shell morphology, *Physical Review B*, **71** (2005) 134406.
- [68] R.C. O'Handley, Soft magnetic materials, *Modern Magnetic Materials*, (2000).
- [69] C. Binns, *Introduction to nanoscience and nanotechnology*, John Wiley & Sons, 2010.
- [70] <https://www.britannica.com/technology/transmission-electron-microscope/images-videos>.
- [71] <http://www.tutorvista.com/content/chemistry/chemistry-iv/solid-state/x-ray-crystals.php>.
- [72] <http://physics.tutorcircle.com/waves/wave-interference.html>
- [73] <http://hyperphysics.phy-astr.gsu.edu/hbase/quantum/bragg.html>.
- [74] <http://www.engr.sjsu.edu/rkwok/squid.htm>.
- [75] <https://www.wmi.badw.de/methods/squid.htm>
- [76] K. Nadeem, H. Krenn, M. Shahid, I. Letofsky-Papst, Influence of SiO_2 matrix and annealing time on properties of Ni-ferrite nanoparticles, *Solid State Sciences*, **19** (2013) 27-31.
- [77] K.H. Wu, Y.C. Chang, G.P. Wang, Preparation of NiZn ferrite/ SiO_2 nanocomposite powders by sol-gel auto-combustion method, *J. Magn. Magn. Mater.*, **269** (2004) 150-155.

- [78] A. Chaudhuri, M. Mandal, K. Mandal, Preparation and study of NiFe₂O₄/SiO₂ core-shell nanocomposites, *J. Alloys Compd.*, **487** (2009) 698-702.
- [79] Z. Zi, Y. Sun, X. Zhu, Z. Yang, J. Dai, W. Song, Synthesis and magnetic properties of CoFe₂O₄ ferrite nanoparticles, *J. Magn. Mater.*, **321** (2009) 1251-1255.
- [80] E.V. Gopalan, P. Joy, I. Al-Omari, D.S. Kumar, Y. Yoshida, M. Anantharaman, On the structural, magnetic and electrical properties of sol-gel derived nanosized cobalt ferrite, *J. Alloys Compd.*, **485** (2009) 711-717.
- [81] T. Krenke, M. Acet, E.F. Wassermann, X. Moya, L. Mañosa, A. Planes, Ferromagnetism in the austenitic and martensitic states of Ni-Mn-In alloys, *Physical Review B*, **73** (2006) 174413.
- [82] G. Lawes, B. Melot, K. Page, C. Ederer, M. Hayward, T. Proffen, R. Seshadri, Dielectric anomalies and spiral magnetic order in CoCr₂O₄, *Physical Review B*, **74** (2006) 024413.
- [83] O. Kahn, Condensed-matter physics: The magnetic turnabout, *Nature*, **399** (1999) 21-22.
- [84] S.-i. Ohkoshi, S. Yorozu, O. Sato, T. Iyoda, A. Fujishima, K. Hashimoto, Photoinduced magnetic pole inversion in a ferro-ferrimagnet: (Fe_{0.40} II Mn_{0.60} II) 1.5 Cr III (CN) 6, *Applied Physics Letters*, **70** (1997) 1040-1042.
- [85] J. Plocek, P. Holec, S. Kubickova, B. Pacakova, I. Matulkova, A. Mantlikova, I. Nemecek, D. Niznansky, J. Vejpravova, Stabilization of Transition Metal Chromite Nanoparticles in Silica Matrix, (2014).
- [86] R. Plumier, Reinvestigation of magnetic structures of CoCr₂O₄ and MnCr₂O₄ obtained by neutron diffraction, *J. Appl. Phys.* **39** (1968) 635-636.
- [87] N. Muftic, A. Nugroho, G. Blake, T. Palstra, Magnetodielectric coupling in frustrated spin systems: the spinels MCr₂O₄ (M= Mn, Co and Ni), *J. Phys: Condensed Matter*, **22** (2010) 075902.
- [88] Z. Tang, J. Chen, C. Sorensen, K. Klabunde, G. Hadjipanayis, Tang et al. reply, *Physical Review Letters*, **68** (1992) 3114.
- [89] K. Binder, Statistical mechanics of finite three-dimensional Ising models, *Physica*, **62** (1972) 508-526.
- [90] P. Tartaj, T. González-Carreño, C.J. Serna, Magnetic behavior of γ-Fe₂O₃ nanocrystals dispersed in colloidal silica particles, *J. Phys. Chem B*, **107** (2003) 20-24.